JHEP

Published for SISSA by Springer

Received: November 6, 2012
Accepted: December 20, 2012
Published: January 18, 2013

Perturbative expansion of τ hadronic spectral function moments and α_s extractions

Martin Beneke,[a] **Diogo Boito**[a] **and Matthias Jamin**[b]

[a] *Physik Department T31, Technische Universität München, James-Franck-Straße 1, D-85748 Garching, Germany*
[b] *Institució Catalana de Recerca i Estudis Avançats (ICREA), IFAE, Theoretical Physics Group, UAB, E-08193 Bellaterra, Barcelona, Spain*

E-mail: diogo.boito@tum.de

Abstract: Various moments of the hadronic spectral functions have been employed in the determination of the strong coupling α_s from tau decays. In this work we study the behaviour of their perturbative series under different assumptions for the large-order behaviour of the Adler function, extending previous work on the tau hadronic width. We find that the moments can be divided into a small number of classes, whose characteristics depend only on generic features of the moment weight function and Adler function series. Some moments that are commonly employed in α_s analyses from τ decays should be avoided because of their perturbative instability. This conclusion is corroborated by a simplified α_s extraction from individual moments. Furthermore, under reasonable assumptions for the higher-order behaviour of the perturbative series, fixed-order perturbation theory (FOPT) provides the preferred framework for the renormalization group improvement of all moments that show good perturbative behaviour. Finally, we provide further evidence for the plausibility of the description of the Adler function in terms of a small number of leading renormalon singularities.

Keywords: Renormalization Group, QCD, Renormalization Regularization and Renormalons

doi:10.1007/JHEP01(2013)125

JHEP01(2013)125

Contents

JHEP01(2013)125

1 Introduction

The precise determination of fundamental parameters of the Standard Model (SM) provides one of the most important tests of its internal consistency. In the strong sector, the QCD coupling α_s plays a prominent role and much effort has been devoted to its extraction from various observables. The determination from τ decays is important, since it provides an accurate extraction at low energies, close to the limit of validity of perturbative QCD.

The general framework for the determination of α_s from the ratio

$$R_\tau \;=\; \frac{\Gamma\left[\tau^- \to \nu_\tau \text{hadrons}(\gamma)\right]}{\Gamma\left[\tau^- \to \nu_\tau e^- \bar{\nu}_e(\gamma)\right]} \;=\; 3.6280 \pm 0.0094 \;\; [1] \tag{1.1}$$

was developed about 20 years ago [2]. Theoretically, R_τ can be expressed as a weighted integral of the measured hadronic spectral functions that runs over the hadronic invariant mass squared s of the hadronic final state from threshold up to m_τ^2. The relevant weight function, $w_\tau(x)$, is obtained from the kinematics of the decay. However, the use of QCD at

very low energies is impractical. Therefore, one resorts to a finite-energy sum rule (FESR) where the theoretical counter-part of R_τ is evaluated as a contour integral in the complex-energy plane with $|s| = m_\tau^2$. A particularity of this observable is that non-perturbative effects, although small, cannot be neglected. The perturbative QCD result must be supplemented with power corrections organised in an operator product expansion (OPE). With the data from the ALEPH [3–5] and OPAL [6] collaborations, as well as progress on the theory side, the precision on $\alpha_s(m_\tau)$ is impressive: the advocated uncertainties that two decades ago were around 11% [2], are now of the order of 2.5% [5] for the most optimistic analysis. However, the results obtained by different groups are sometimes barely compatible, which suggests that the details of the different analyses need to be scrutinised.

In the theoretical description two ingredients are needed. The first of them is the perturbative QCD contribution, the second are the non-perturbative effects. At present, two theoretical obstacles obstruct progress on the theory side. First, the renormalisation group improvement of the perturbative series remains controversial — we return to this subject below. Second, the treatment of non-perturbative effects (encoded in the OPE) in some of the existent analyses was shown to be inconsistent [7]. A possible solution to this problem, proposed in [7–9], is the inclusion of the so-called duality violations (DVs) in the analysis framework. These are related to the fact that the OPE fails to describe the spectral functions near the Minkowski axis, where resonance effects may become important and local quark-hadron duality is violated. In the past, the standard assumption was that DVs could be disregarded due to the kinematical suppression of contributions from this problematic region. Progress in modelling DVs [10–16] made it possible to include them in the α_s analyses without reliance on external input [8, 9], and to test the above assumption.

In the present work we focus on the perturbative contribution. One of the main sources of uncertainty in the theory of hadronic τ decays is the renormalisation group (RG) improvement of the perturbative series. The most widely employed prescriptions are fixed-order perturbation theory (FOPT, see for instance ref. [17, 18]) and contour-improved perturbation theory (CIPT) [19, 20]. Employing these prescriptions at a finite order in perturbation theory leads to differing values for α_s. The inclusion of the recently computed α_s^4 correction [21] to R_τ rendered the discrepancy between FOPT and CIPT even more pronounced. Since then, several works have dealt with the RG improvement of the series [18, 22–26]. A difficulty common to all these works is that conclusions in favour of FOPT or CIPT (or a third prescription) depend on implicit or explicit assumptions on the yet unknown higher order coefficients of the Adler function. In particular, the aim of ref. [18] was to construct a plausible model for the perturbative series in higher orders incorporating only general features of the leading renormalon singularities of the Borel-transformed Adler function. This should be sufficient to describe the perturbative coefficients at intermediate and high orders, augmented by some polynomial terms to take care of the first few coefficients which are not yet dominated by (pre-)asymptotic behaviour. After matching of the model to the known coefficients of the Adler function in QCD, the main conclusion of ref. [18] was that FOPT is to be preferred over CIPT, since at order α_s^4 and in the region of its smallest terms, FOPT provides a closer approach to the resummed series than CIPT.

JHEP01(2013)125

How general is this conclusion? A short-coming of ref. [18] and other recent works (with the exception of ref. [24]) is that the analysis was done solely for the kinematical weight w_τ. This is not entirely satisfactory because the α_s determinations employ — and often require — several different weight functions, if only to extract α_s together with the non-perturbative condensates and DV parameters from the same self-consistent analysis. In fact, any analytic weight function $w_i(x)$ gives rise to a valid FESR, and different $w_i(x)$ emphasise different energy regions of the experimental data and different contributions of the theoretical description. In the analyses of α_s found in the literature, several different moments have been used. The enhancement or the suppression of condensates and DV contributions have been the guiding principle in choosing these moments. Still, little attention has been devoted to the moment dependence of the convergence properties of the perturbative series and we aim to fill this gap here. In the present paper we therefore pursue the FOPT/CIPT comparison using the methods of ref. [18], and ask whether the preference for one or the other depends on specific features of the weight function, or the assumptions on the Adler function coefficients; whether the kinematic weight is special, or all moments are alike.

The outline is as follows. After setting up the necessary notation, we study how the convergence properties of the perturbative expansion depend on the choice of the weight function that defines the moment. We try, as much as possible, to remain model independent by making use not only of the reference model of ref. [18], but also employing an extreme case where CIPT is, by construction, preferred over FOPT for the kinematical weight function. We show that with respect to convergence properties and the FOPT/CIPT comparison the moments can be divided into several classes, whose global features are manifestations of simple properties of the weight functions and assumptions on the Adler function series. We conclude that certain weight functions should be more suitable for α_s analyses than others. We then study the robustness of the model proposed in ref. [18] in the light of the criticism presented in ref. [24] and provide further plausibility arguments in favour of the adopted procedure. Finally, in the last section we study the consistency between the moments by performing simplified α_s determinations from single-moment fits.

2 Theoretical framework

The total decay rate of the τ lepton into hadrons, eq. (1.1), can be separated experimentally into three components: the vector, $R_{\tau,V}$, and axial-vector, $R_{\tau,A}$, arising from the decays into light quarks through the $(\bar{u}d)$-quark current, and contributions with net strangeness, $R_{\tau,S}$, from the $(\bar{u}s)$-quark current. Hence

$$R_\tau \;=\; R_{\tau,V} + R_{\tau,A} + R_{\tau,S}\,. \tag{2.1}$$

In determinations of α_s, the focus is on the non-strange contributions, because power corrections are largest in the strange sector, while they are suppressed by the light u- and d-quark masses for $R_{\tau,V}$ and $R_{\tau,A}$. For this reason, in the following we restrict ourselves to the two latter channels.

JHEP01(2013)125

The ratios $R_{\tau,V/A}$ can be expressed in terms of integrals of the spectral functions $\mathrm{Im}\,\Pi^{(1)}_{V/A}$ and $\mathrm{Im}\,\Pi^{(0)}_{V/A}$ as

$$R_{\tau,V/A} \;=\; 12\pi S_{\rm EW}|V_{ud}|^2 \int\limits_0^{m_\tau^2} \frac{ds}{m_\tau^2}\left(1-\frac{s}{m_\tau^2}\right)^2\left[\left(1+2\frac{s}{m_\tau^2}\right)\mathrm{Im}\,\Pi^{(1)}_{V/A}(s)+\mathrm{Im}\,\Pi^{(0)}_{V/A}(s)\right]. \quad (2.2)$$

In the last equation, $S_{\rm EW}$ is an electroweak correction [27–29], and V_{ud} is the quark-mixing matrix element [30]. Theoretically, the relevant two-point functions whose spectral functions enter eq. (2.2) are

$$\Pi^{\mu\nu}_{V/A}(p) \;\equiv\; i\int dx\, e^{ipx}\,\langle\Omega|\,T\{J^\mu_{V/A}(x)\,J^\nu_{V/A}(0)^\dagger\}|\Omega\rangle\,, \quad (2.3)$$

with $|\Omega\rangle$ being the physical vacuum, and the V and A currents are $J^\mu_{V/A}(x)=(\bar u\gamma^\mu(\gamma_5)d)(x)$. These correlators assume the standard decomposition into transversal and longitudinal components which was employed in writing eq. (2.2).

One then makes use of the fact that the exact correlation functions are analytic in the complex s-plane except for a cut along the real axis. This property allows one to write eq. (2.2) as a counter-clockwise contour integral along the circle $|s|=s_0$

$$R^{w_i}_{V/A}(s_0) \;=\; 6\pi i\, S_{\rm EW}|V_{ud}|^2 \oint\limits_{|s|=s_0} \frac{ds}{s_0}\,w_i\,(s)\left[\Pi^{(1+0)}_{V/A}(s)+\frac{2s}{(s_0+2s)}\,\Pi^{(0)}_{V/A}(s)\right]. \quad (2.4)$$

In writing the last equation we have performed two generalisations. First, we are using a generalised analytic weight function $w_i(s)$, second, the integral is performed up to an arbitrary energy $s_0\le m_\tau^2$. In the notation of eq. (2.4), the particular case of eq. (2.2) corresponds to $R^{w_\tau}_{V/A}(m_\tau^2)$ with $s_0=m_\tau^2$ and

$$w_\tau(s) \;=\; \left(1-\frac{s}{m_\tau^2}\right)^2\left(1+2\frac{s}{m_\tau^2}\right). \quad (2.5)$$

For large enough s, the contributions to $\Pi^{(J)}(s)$ can be organised in an operator product expansion: a series of local gauge-invariant operators of increasing dimensions times the appropriate inverse powers of s. In this framework, the purely perturbative part in the chiral limit can be associated with the dimension-zero operator, whereas dimension-2 contributions arise from the quark mass corrections.[1] The first non-trivial operators arise at dimension 4, namely, the quark and gluon condensates. The OPE is expected to be well behaved along the contour $|s|=s_0$ (for s_0 sufficiently large) except close to the positive real axis. Therefore, in the general case, $R^{w_i}_{V/A}(s_0)$ obtains a contribution from corrections due to the break-down of the OPE close to real $s>0$. This term is the aforementioned DV contribution. Weight functions $w_i(s)$ that contain one or more zeros at $s=s_0$, such as the kinematical w_τ in eq. (2.5), tend to suppress the contribution of DVs.

The different components of $R^{w_i}_{V/A}$ can be collected in the following expression

$$R^{w_i}_{V/A}(s_0) \;=\; \frac{N_c}{2}\,S_{EW}|V_{ud}|^2\left[\delta^{\rm tree}_{w_i}+\delta^{(0)}_{w_i}(s_0)+\sum_{D\ge 2}\delta^{(D)}_{w_i,V/A}(s_0)+\delta^{\rm DV}_{w_i,V/A}(s_0)\right]. \quad (2.6)$$

[1] In the case at hand, namely u and d quarks only, the dimension-2 corrections are tiny.

JHEP01(2013)125

In the last equation, $\delta^{\rm tree}_{w_i}$ and $\delta^{(0)}_{w_i}$ are the perturbative terms,[2] of which $\delta^{(0)}_{w_i}$ contains the α_s corrections. Since $\delta^{\rm tree}_{w_i}$ and $\delta^{(0)}_{w_i}$ do not depend on the flavour, in the chiral limit they are the same for vector and axial-vector correlators, and correspond to the perturbative series for the correlator $\Pi^{(1+0)}_{V/A}(s)$. The contributions from the quark masses, as well as that of the operators with $D > 2$, are encoded in the terms $\delta^{(D)}_{w_i,V/A}$, while the DV contributions are represented by $\delta^{\rm DV}_{w_i,V/A}$. In this work we are interested in the convergence properties of the purely perturbative corrections, and thus our focus is on $\delta^{(0)}_{w_i}$.

The correlator $\Pi^{(1+0)}$ is not RG invariant and contains scale- and scheme-dependent contributions. However, the Cauchy integral in eq. (2.4) is insensitive to all s-independent terms in the correlators. Without loss of generality, one can work with a renormalisation invariant quantity, known as the Adler function, and defined through

$$D^{(1+0)}(s) \equiv -s\,\frac{d}{ds}\,\Pi^{(1+0)}(s)\,. \tag{2.7}$$

Using partial integration, and performing the substitution $x = s/s_0$, one can write

$$\delta^{(0)}_{w_i} = -2\pi i \oint\limits_{|x|=1} \frac{dx}{x}\, W_i(x)\, D^{(1+0)}_{\rm pert}(s_0 x)\,, \tag{2.8}$$

where "pert" denotes the perturbative part of the Adler function in the chiral limit and the weight function $W_i(x)$ is obtained from $w_i(x)$ by the integral $W_i(x) = 2\int_x^1 dz\, w_i(z)$.

In full generality, the perturbative Adler function admits the following expansion:

$$D^{(1+0)}_{\rm pert}(s) = \frac{N_c}{12\pi^2}\sum_{n=0}^{\infty} a_\mu^n \sum_{k=1}^{n+1} k\, c_{n,k}\, L^{k-1}\,, \qquad L \equiv \log\frac{-s}{\mu^2}\,, \tag{2.9}$$

with $a_\mu \equiv a(\mu^2) \equiv \alpha_s(\mu)/\pi$, μ is the renormalisation scale, and N_c the number of colours. Imposing the RG invariance of the above equation, one may consider as independent only the coefficients $c_{n,1}$. The other coefficients $c_{n,k}$, with $k = 2, 3, \ldots, n+1$, can be obtained in terms of the $c_{n,1}$ and β-function coefficients.[3] (Explicit expressions for some of the coefficients $c_{n,k}$ can be found in eq. (2.11) of ref. [18].) At $N_c = N_f = 3$ the numerical values of the known coefficients $c_{n,1}$ are

$$c_{0,1} = c_{1,1} = 1\,, \quad c_{2,1} = 1.640\,, \quad c_{3,1} = 6.371\,[31, 32]\,, \quad c_{4,1} = 49.076\,[21]\,. \tag{2.10}$$

Fully analytic results for the coefficients can be found in ref. [21]. Based on a geometrical growth of the terms in the perturbative expansion of $\delta^{(0)}_{w_\tau}$, in ref. [18] the estimate

$$c_{5,1} \approx 283 \tag{2.11}$$

was put forward for the next term in the series. This estimate was corroborated by the model introduced in ref. [18] and we will also employ it in our work.

[2] Henceforth, we omit the s_0 dependence in the terms of the r.h.s. of eq. (2.6).

[3] We follow the convention of ref. [18], i.e. $\beta(a_\mu) \equiv \mu da_\mu/d\mu = \sum_{k=1}\beta_k a_\mu^{k+1}$. The first coefficient is then $\beta_1 = 11N_c/6 - N_f/3$.

JHEP01(2013)125

Inserting the general expansion of the Adler function, eq. (2.9), into the expression for $\delta_{w_i}^{(0)}$, eq. (2.8), yields

$$\delta_{w_i}^{(0)} = \sum_{n=1}^{\infty}\sum_{k=1}^{n} k\, c_{n,k}\, \frac{1}{2\pi i}\oint\limits_{|x|=1}\frac{dx}{x}\, W_i(x)\log^{k-1}\left(\frac{-s_0 x}{\mu^2}\right) a_\mu^n\,. \tag{2.12}$$

Since the Adler function satisfies a homogeneous RG equation, the above expression for $\delta_{w_i}^{(0)}$ is μ-independent. One has the freedom of setting the scale μ in a convenient way.

The fixed-order prescription corresponds to $\mu^2 = s_0$. In this case, the coupling is calculated at a fixed scale and can be taken outside the integral. However, the logarithms remain to be integrated along the contour. The result can be cast into

$$\delta_{\mathrm{FO},w_i}^{(0)} = \sum_{n=1}^{\infty} a(s_0)^n \sum_{k=1}^{n} k\, c_{n,k}\, J_{k-1}^{\mathrm{FO},w_i}\,, \tag{2.13}$$

where the integrals are given by

$$J_n^{\mathrm{FO},w_i} \equiv \frac{1}{2\pi i}\oint\limits_{|x|=1}\frac{dx}{x}\, W_i(x)\log^n(-x)\,. \tag{2.14}$$

For polynomial moments, these integrals can be performed analytically. Explicit expressions for the particular case of the kinematic weight function can be found in ref. [18].

In contour-improved perturbation theory [19, 20], the logarithms that remain in the FO prescription are summed with the choice $\mu^2 = -s_0 x$ before calculating the contour integral. This procedure implies that the contour integrals have to be performed over the running α_s in the complex plane

$$\delta_{\mathrm{CI},w_i}^{(0)} = \sum_{n=1}^{\infty} c_{n,1}\, J_n^{\mathrm{CI},w_i}(s_0)\,, \tag{2.15}$$

where the integrals, that can only be computed numerically, are given by

$$J_n^{\mathrm{CI},w_i}(s_0) \equiv \frac{1}{2\pi i}\oint\limits_{|x|=1}\frac{dx}{x}\, W_i(x)\, a^n(-s_0 x)\,. \tag{2.16}$$

CIPT resums the running of the QCD coupling along the contour of integration. Consequently, at each order n, only the coefficient $c_{n,1}$ enters the expression.

3 Models for the Adler function

In order to discuss the behaviour of the perturbative expansion of the spectral moments and to compare FO to CI perturbation theory, we need an ansatz for the coefficients $c_{n,1}$ of the Adler function, which is the dynamical input common to all moments, beyond $n = 4$. In this section we introduce the models for the series that we use later on. A caveat needs to be spelled out at this point. Going beyond the exactly known coefficients $c_{n,1}$ requires

JHEP01(2013)125

assumptions, usually based on some form of regularity of the series, which might simply be wrong. The series might have outliers at some order, and we will never know. The best we can do is to state the assumptions clearly, to provide supporting arguments where they exist, and to explore the consequences. Two diverging assumptions may be distinguished:

- The high-order coefficients $c_{n,1}$ beyond $n = 4$ are not important, and can be neglected. The RG improvement still generates a non-trivial series expansion of the spectral moments to all orders through the dependence of $c_{n,k}$ with $k > 1$ on the known $c_{n,1}$. In a sense this is the assumption underlying CIPT, which assumes that the running coupling terms are dominant and therefore should be summed.

- The high-order coefficients $c_{n,1}$ beyond $n = 4$ are essential, since they diverge factorially for large n, thus overcoming the geometric growth of the running coupling terms. Since some knowledge exists on the general structure of this divergence (reviewed in ref. [33]), this information can and should be included.

The two main models that we discuss in this section can be viewed as representatives of these assumptions. In addition we also briefly review the result in the large-β_0 approximation,[4] which, since it is based on a well-defined formal limit ($N_f \to -\infty$) of QCD, provides a useful toy model to which we shall return in section 5. In the context of tau decays, this toy model has been studied in refs. [34, 35].

We start by giving a number of definitions and establishing the notation. We define a new function $\widehat{D}(s)$ related to the Adler function by

$$\frac{12\pi^2}{N_c}\, D_V^{(1+0)}(s) \;\equiv\; 1 + \widehat{D}(s) \;\equiv\; 1 + \sum_{n=0}^{\infty} r_n\, \alpha_s(\sqrt{s})^{n+1}\,. \tag{3.1}$$

The coefficients $c_{n,1}$ of $D_V^{(1+0)}$ are related to those of $\widehat{D}(s)$ by $c_{n,1} = \pi^n r_{n-1}$. The Borel transform of the above series is defined by

$$B[\widehat{D}](t) \;\equiv\; \sum_{n=0}^{\infty} r_n\, \frac{t^n}{n!}\,. \tag{3.2}$$

One can then define the Borel integral of the series as (α positive)

$$\widehat{D}(\alpha) \;\equiv\; \int_0^{\infty} dt\, \mathrm{e}^{-t/\alpha}\, B[\widehat{D}](t)\,, \tag{3.3}$$

which has the same series expansion in α as $\widehat{D}(s)$ has in $\alpha_s(\sqrt{s})$. The last integral, $\widehat{D}(\alpha)$, if it exists, gives the Borel sum of the original divergent series eq. (3.1). An important point in the case of the Adler function is that $B[\widehat{D}](t)$ contains singularities on the positive real axis which forces one to adopt a procedure to define the integral $\widehat{D}(\alpha)$. The choice of the procedure introduces an ambiguity. We discuss this point in more detail below.

[4] For historical reasons, we speak about the "large-β_0" approximation, although in the notation employed in this work, the leading coefficient of the β-function is termed β_1.

JHEP01(2013)125

3.1 Large-β_0 model

In the context of the large-β_0 approximation, it has been shown by resumming bubble-chain diagrams that the Borel-transformed Adler function has infrared (IR) and ultraviolet (UV) renormalon poles at positive and negative integer values of the variable $u = \beta_1 t/(2\pi)$, respectively [36, 37]. (Except at the value $u = 1$.) The IR renormalon poles are related to the power corrections in the OPE, while the leading UV renormalon dictates the large-order behaviour of the series. (For a review see ref. [33]).

The main result of refs. [36, 37] is that in the large-β_0 approximation the Borel transformed Adler function can be written as [37]

$$B[\widehat{D}](u) \;=\; \frac{32}{3\pi}\,\frac{\mathrm{e}^{-Cu}}{(2-u)}\,\sum_{k=2}^{\infty}\frac{(-1)^k k}{[k^2-(1-u)^2]^2}\,, \tag{3.4}$$

where the constant C is scheme dependent and cancels the scheme dependence of α_s in eq. (3.3), such that $\widehat{D}(s)$ is scheme independent. (In the $\overline{\text{MS}}$-scheme $C = -5/3$.) In large-β_0, all the UV renormalon poles at $u = -1, -2, \ldots$, are double poles, as are all the IR poles at $u = 3, 4, \ldots$. The only exception is the IR pole at $u = 2$, which is simple. This follows from the fact that the operator $\alpha_s GG$ has no anomalous dimension in the large-N_f limit. The absence of an IR renormalon pole at $u = 1$ stems from the fact that no dimension-2 operator contributes to the OPE. The coefficients $c_{n,1}$ in this case can be obtained from eq. (3.4) by expanding in u and performing the Borel integral term by term. The first 12 coefficients can be found in table 1 of ref. [18]. An interesting feature of the large-β_0 result, in apparent coincidence with the full QCD series (2.10), is that the asymptotically dominant sign-alternation from the UV pole at $u = -1$ is delayed in the conventionally adopted $\overline{\text{MS}}$-scheme. In intermediate orders the series coefficients are governed by the fixed-sign contributions from the $u = 2$ pole, whose residue is a factor e^{-3C} larger.

3.2 Reference model

In full QCD we do not have the equivalent of eq. (3.4). On the other hand, the structure of the OPE and general RG arguments allow one to determine the position and strength of the singularities, which evolve from poles into branch cuts [18, 38, 39], though not their residues. In general, the IR and UV singularities are described by the following structures

$$\begin{aligned} B[\widehat{D}_p^{\text{IR}}](u) \;&\equiv\; \frac{d_p^{\text{IR}}}{(p-u)^{1+\tilde{\gamma}}}\left[1+\tilde{b}_1(p-u)+\tilde{b}_2(p-u)^2+\cdots\right], \\ B[\widehat{D}_p^{\text{UV}}](u) \;&\equiv\; \frac{d_p^{\text{UV}}}{(p+u)^{1+\bar{\gamma}}}\left[1+\bar{b}_1(p+u)+\bar{b}_2(p+u)^2+\cdots\right], \end{aligned} \tag{3.5}$$

where the constants $\tilde{\gamma}$, $\tilde{b}_i$, $\bar{\gamma}$, and $\bar{b}_i$ of a pole at p depend on anomalous dimensions of operators in the OPE as well as β-function coefficients (the explicit expressions are given in section 5 of ref. [18]). When performing the integral (3.3) one needs to circumvent the IR singularities along the real axis. A prescription to define the integral is needed which introduces an ambiguity in the Borel resummed result. The ambiguity is expected to be cancelled by exponentially small terms in α_s or, due to the running of the coupling, by

JHEP01(2013)125

power corrections. The treatment of the Borel integral in the presence of these singularities is discussed in appendix A of [18].

The model for the Adler function constructed in ref. [18] (henceforth called *reference model*, or simply RM) is based on the assumption that it makes sense to merge the exactly known low-order behaviour to the leading and sub-leading asymptotics generated by singularities of the Borel transform. Since the known coefficients do not display the asymptotic sign alternating pattern, the leading, first UV singularity should be sufficient. On the other hand, if the intermediate orders are governed by fixed-sign behaviour, at least the first two IR renormalon singularities should be included in the model. Based on these considerations, the ansatz reads

$$B[\widehat{D}](u) \;=\; B[\widehat{D}_1^{\rm UV}](u) + B[\widehat{D}_2^{\rm IR}](u) + B[\widehat{D}_3^{\rm IR}](u) + d_0^{\rm PO} + d_1^{\rm PO}\, u\,, \tag{3.6}$$

where the renormalon singularities are described by the formulae of eq. (3.5).

This ansatz is then matched to the known coefficients of the Adler function in QCD as follows. First, the known coefficients $c_{3,1}$, $c_{4,1}$, and the estimated coefficient $c_{5,1}$, are used to fix the residua of the three renormalon singularities. The polynomial terms are then fixed in order to reproduce the lowest order coefficients $c_{1,1}$ and $c_{1,2}$. The resulting parameters are given in eq. (6.2) of [18] and the first line of table 3 in section 5, and take "reasonable" values. One is then in a position to perform the Borel integration in order to ascribe a resummed value to the asymptotic Adler function series. The higher-order coefficients $c_{n,1}$ can be derived and the behaviour of FOPT and CIPT series can be compared to the resummed one.

The main conclusion of ref. [18] is that under the above assumptions FOPT is clearly preferred over CIPT for w_τ. The CIPT series displays a faster convergence but fails to give a good approximation to the Borel resummed result in the sense of an asymptotic series. From FOPT, on the other hand, it is possible to extract a good approximation to the Borel resummed value in spite of the slower convergence of the series. The reason for this observation can be traced back to cancellations that are missed by the CIPT series. To understand this we rewrite $\delta^{(0)}_{{\rm FO},w_i}$ of eq. (2.13) as

$$\delta^{(0)}_{{\rm FO},w_i} \;=\; \sum_{n=1}^{\infty} \Big[c_{n,1}\delta_{w_i}^{\rm tree} + g_n^{[w_i]}\Big]\, a(s_0)^n\,, \tag{3.7}$$

with

$$g_n^{[w_i]} \;=\; \sum_{k=2}^{n} k\, c_{n,k} J_{k-1}^{{\rm FO},w_i}\,. \tag{3.8}$$

The $c_{n,1}$ series is simply the Adler function series multiplied by $\delta_{w_i}^{\rm tree}$, while the contour integration of the running coupling effects is fully contained in the $g_n^{[w_i]}$ series. In eq. (3.7) the tree-level contribution arises because $J_0^{{\rm FO},w_i} = W_i(0) = \delta_{w_i}^{\rm tree}$. FOPT treats the $c_{n,1}$ and the $g_n^{[w_i]}$ series on an equal footing. Comparing this decomposition with the CIPT result, eq. (2.15), one observes that in CIPT the $g_n^{[w_i]}$ series is resummed to all orders while the $c_{n,1}$ series is used only up to a finite order n. An important model-independent

JHEP01(2013)125

	Reference model			Alternative model		
n	c_n	$g_n^{[w_\tau]}$	$(c_n + g_n^{[w_\tau]})/c_n$	c_n	$g_n^{[w_\tau]}$	$(c_n + g_n^{[w_\tau]})/c_n$
4	49.1	78.0	2.59	49.1	78.0	2.59
5	283	307.8	2.09	283	307.8	2.09
6	3275.4	−807.3	0.75	2148.3	−807.3	0.62
7	18, 758	−10, 398	0.45	11, 801	−34, 489	−1.92
8	388, 442	−329, 054	0.15	150, 508	−592, 196	−2.93
9	919, 121	−232, 718	0.75	215, 264	-5.1×10^6	−22.8
10	8.4×10^7	-7.3×10^7	0.12	2.4×10^7	-6.4×10^7	−1.69

Table 1. Cancellations between the c_n and the $g_n^{[w_\tau]}$ series for orders $4 \leq n \leq 10$ for the kinematical moment, w_τ, in the reference model and in the alternative model, eqs. (3.6) and (3.9).

feature of the QCD series, which follows from the OPE and the form of the moment weight function, is that there are large cancellations of $n!$ divergences between the $c_{n,1}$ and $g_n^{[w_i]}$ series. These cancellations are particularly strong when the series is dominated by the $u = 2$ singularity, and for the kinematic weight.[5] In such a scenario, it is mandatory to combine $c_{n,1}$ and $g_n^{[w_i]}$ order by order in n, lest the cancellations do not take place. Since CIPT treats the orders incoherently, it misses the cancellations and runs into the sign alternating asymptotic regime earlier. In FOPT, on the other hand, the cancellations suppress the divergence and allow FOPT to approach the Borel result. In table 1, we show as an example the cancellations in the case of the kinematical moment w_τ. However, note that they are not imposed in the RM. Rather, the matching procedure to the QCD series gives the expected weight to the leading IR pole. If the residue of the IR pole $u = 2$ had turned out to be tiny, this would have made the cancellations almost non-existent.

3.3 Alternative model

To make this feature clearer, we can *artificially* suppress the leading IR pole. Let us consider a model for the Borel transformed Adler function where the IR singularity at $u = 2$ is removed and another at $u = 4$ is added:

$$B[\widehat{D}](u) \;=\; B[\widehat{D}_1^{\rm UV}](u) + B[\widehat{D}_3^{\rm IR}](u) + B[\widehat{D}_4^{\rm IR}](u) + d_0^{\rm PO} + d_1^{\rm PO}\, u\,. \tag{3.9}$$

In this model, the aforementioned cancellations do not take place by construction. We refer to this model as the *alternative model* (AM). An analogous matching procedure can be carried out yielding the following values for the parameters:

$$\begin{aligned} d_3^{\rm IR} &= 66.18\,, & d_4^{\rm IR} &= -289.71\,, & d_1^{\rm UV} &= -5.21\times 10^{-3}\,,\\ d_0^{\rm PO} &= 2.15\,, & d_1^{\rm PO} &= 4.01\times 10^{-1}\,. \end{aligned} \tag{3.10}$$

[5] In large-β_0 this is shown analytically for w_τ in ref. [18]. An important point discussed in the next section is the moment dependence of the cancellations.

JHEP01(2013)125

Here, as we show in the sequel, CIPT is able to approach the Borel resummed result while FOPT exhibits oscillations around this value. Table 1 shows that the cancellations between the c_n and $g_n^{[w_i]}$ series no longer take place in this model. The table also shows a slower growth of the $c_{n,1}$ in this model, and a dominance of the g_n terms up to $n = 10$, which therefore realises a situation where running coupling effects are dominant. We use this model as an example where CIPT is, by construction, superior to FOPT, at least for the kinematical weight. This provides a way to assess a possible model dependence in our conclusions. Nevertheless, we emphasise that we find it unlikely that the Adler function in QCD behaves as the AM, since there is no known mechanism that would naturally suppress the $u = 2$ singularity.

4 Moment analysis

The determination of α_s and condensates from the analysis of τ hadronic spectral functions is based on sum rules obtained by equating eqs. (2.2) and (2.4). In the former, to perform the integral along the real axis, the experimental spectral functions are used. In eq. (2.4), the theoretical description of the correlators is employed in the contour integration. An important aspect of these sum rules is that one still has the freedom of choosing any analytic weight function $w_i(x)$, as well as any point $s_0 \leq m_\tau^2$ (as long as s_0 is large enough for the OPE and the perturbative expansion to make sense). On the experimental side, it is obvious that a given weight function enhances the regions of the spectrum where it has peaks. On the theory side, the relative contributions of the different δ's in eq. (2.6) are strongly dependent on the choice of $w_i(x)$. For example, as already mentioned, moments of functions w_i with zeros at $s = s_0$ suppress $\delta_{w_i}^{\rm DV}$. These are known in the literature under the name *pinched moments*. A monomial term of the type x^k in w_i, on the other hand, implies the monomial x^{k+1} in W_i defined after eq. (2.8), which enhances (or, rather, does not suppress) the contribution of the condensate of dimension $D = 2(k+1)$ as well as the factorial divergence from the IR renormalon singularity at $u = k+1$. Let us analyse, as an illustrative example, the kinematical moment

$$w_\tau \;=\; (1-x)^2(1+2x) = 1 - 3x^2 + 2x^3. \tag{4.1}$$

It receives its larger contributions from $\delta_{w_\tau}^{\rm tree}$, $\delta_{w_\tau}^{(0)}$, $\delta_{w_\tau}^{(6)}$, and $\delta_{w_\tau}^{(8)}$. The first two arise mainly from the 1 in w_τ, whereas $\delta_{w_\tau}^{(6)}$ and $\delta_{w_\tau}^{(8)}$ arise from the terms $-3x^2$ and $2x^3$, respectively. The double zero at $x = 1$ suppresses $\delta_{w_\tau}^{\rm DV}$, while the absence of other monomial terms suppresses the condensates with $D = 4$ as well as with $D \geq 10$. (The mass corrections, $\delta_{w_\tau}^{(2)}$, are negligible due to the smallness of the quark masses.)

In order to extract α_s, a number of condensates, and the DV parameters from the data sets one needs more than one observable. It has become standard to use a set of several weight functions w_i in order to perform a combined fit to their — not statistically independent — moments. In table 2 we collect the weight functions investigated in this work. Most of them have been employed in at least one of the recent analyses of hadronic τ spectral functions. In this table, the first five rows are the building blocks for the other polynomial weight functions. The second set are pinched weight-functions that contain

JHEP01(2013)125

i	$w_i(x)$	$\delta^{\rm tree}_{w_i}$	refs.
1	1	2	[8, 9]
2	x	1	—
3	x^2	2/3	—
4	x^3	1/2	—
5	x^4	2/5	—
6	$1-x$	1	—
7	$1-x^2$	4/3	[8, 9]
8	$1-x^3$	3/2	[8, 9]
9	$1-\frac{3x}{2}+\frac{x^3}{2}$	3/4	[7]
10	$(1-x)^2$	2/3	[7]
11	$(1-x)^3$	1/2	—
12	$(1-x)^2(1+2x)$	1	w_τ
13	$(1-x)^3(1+2x)$	7/10	[5]
14	$(1-x)^2x$	1/6	[7]
15	$(1-x)^3x(1+2x)$	1/6	[5]
16	$(1-x)^3x^2(1+2x)$	13/210	[5]
17	$(1-x)^3x^3(1+2x)$	1/35	[5]

Table 2. Weight functions investigated in this analysis, together with the corresponding $\delta^{\rm tree}_{w_i}$. In the last column, we give the reference to recent works that employed the given weight function in analyses of τ decay data. The kinematical weight function w_τ was used many times throughout the literature and we refrain from quoting all the works that employed it.

a 1 followed by powers of x. The third block contains pinched weight-functions that do not have the 1 and start directly with some power of x. The idea behind the moments that were used in the existent analyses was mainly the enhancement or the suppression of condensates and DV contributions. In combined fits to sets of moments (e.g. refs. [5–9]), the final value of α_s receives contributions from the perturbative terms of all moments employed. Therefore, in order to achieve a trustworthy determination of the coupling, it is desirable to understand the convergence properties of the perturbative component for all the moments employed in the α_s analysis.

In the remainder of this section we study the behaviour of the term $\delta^{(0)}_{w_i}(m_\tau^2)$, for the moments of table 2 in FOPT and CIPT, given by eqs. (2.13) and (2.15) respectively. In doing so, we employ for the coefficient $c_{5,1}$ the estimate of eq. (2.11). Regarding higher orders, two scenarios are considered: the reference model of ref. [18], given in eq. (3.6), and the alternative model of eq. (3.9), which provides an example case where CIPT is better than FOPT for the kinematical weight. In plots for the perturbative series we display the results for both models side by side to facilitate the comparison. The respective Borel

JHEP01(2013)125

resummed values are also shown, together with the Borel ambiguity. Since both models are matched to the first five coefficients, their results for CIPT and FOPT are identical by construction up to the fifth order.

In our analysis, it becomes clear that one can group the 17 different $\delta^{(0)}_{w_i}$ into four classes: the monomial terms, the pinched-weights with a "1" in the weight function, pinched weights without a "1", and all moments that contain the term x, which form a separate category. We analyse these classes in the remainder of this section.

4.1 Building blocks: the monomial terms

Since the weight functions employed are all polynomial, it is instrumental to start the analysis with the monomial terms given in the first 5 entries of table 2.

The first of them, the constant $w_1 = 1$, is quite particular. On the experimental side this moment gives the same weight to the whole spectrum. On the theory side, it obtains very little contribution from condensates, since no powers of x appear, picking up only the logarithmic contributions in the Wilson coefficients of the OPE.[6] The behaviour of $\delta^{(0)}_{w_1}$ for FOPT and CIPT is shown in figure 1(a) for the reference model, and in figure 1(b) for the alternative model. A feature that can be observed in FO is a rapid growth in the first few terms, followed by a decrease in the value of $\delta^{(0)}_{w_1}$. In lower orders, the series overshoots the Borel summed values for both models. Later, FOPT oscillates around the Borel sum. The amplitude of the oscillations are much smaller in the RM, and from order $n = 5$ the series can be considered a good approximation to the true result in the sense of an asymptotic series. The smaller oscillations in the RM model are due to the previously mentioned cancellations among the c_n and the $g_n^{[w_1]}$ series. CIPT is more stable in both cases, but it fails to give a good approximation to the Borel resummed value of the RM. In the case of the alternative model, CIPT is able to approach the true value, as expected. The smallness of the ambiguity of the Borel integral due to the poles on the integration contour (indicated by the horizontal shaded band in the figures) in these cases can be understood since the moment receives only small logarithmic contributions from the condensates in the OPE (for lack of powers of x). Accordingly, the ambiguities of the IR poles are also small.[7]

The behaviour of $\delta^{(0)}_{w_i}$ for the monomials $w_3 = x^2$, $w_4 = x^3$, $w_5 = x^4$ is qualitatively very similar. Therefore, we display only the representative case of x^2 in figures 1(e) and 1(f) for the RM and AM, respectively, which highlights these similarities. We note that the values of $\delta^{(0)}_{w_i}$ are 4 to 6 times smaller than the ones for w_1. This plays an important role in the case of moments with pinching. Finally, w_3 is maximally sensitive to the Borel ambiguity of the IR singularity at $u = 3$, present in both models. However, the residue in the case of the RM is about 5 times smaller than in the AM, which explains the different magnitudes of the shaded bands in the two plots.

The behaviour of the monomial $w_2 = x$ is exceptional, as shown in figure 1(c) for the reference model, and in figure 1(d) for the alternative model. One can separate the

[6] This is precisely the reason why this moment is central to the analysis of refs. [8, 9], where one wants to extract the DVs from data.

[7] They would be zero if the poles were simple. Since we include the four-loop structure for the renormalon singularities, they are small, but non-zero. See appendix A of ref. [18] for the explicit formulae.

JHEP01(2013)125

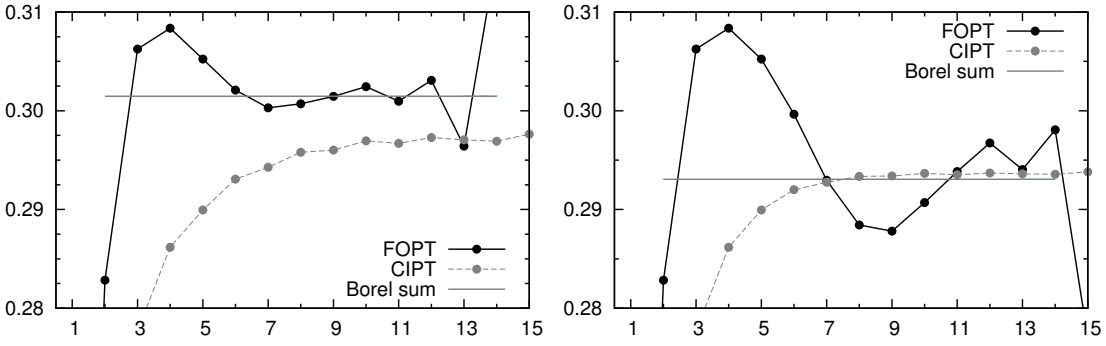

(a) $w_1 = 1$, reference model

(b) $w_1 = 1$, alternative model

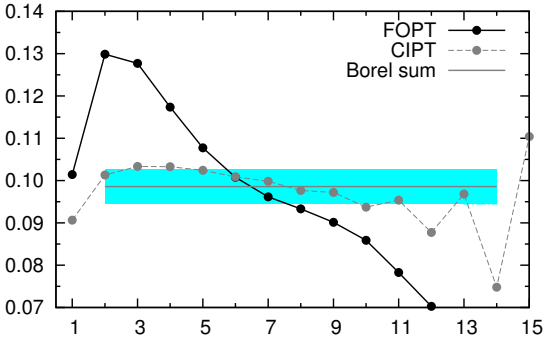

(c) $w_2 = x$, reference model

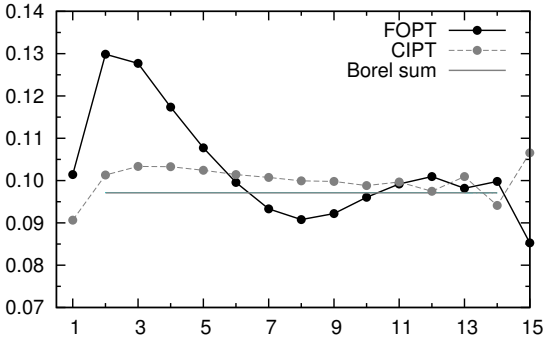

(d) $w_2 = x$, alternative model

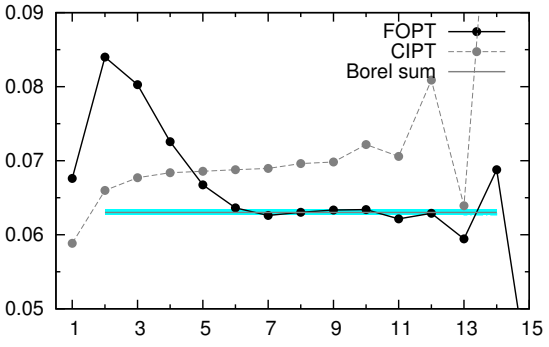

(e) $w_3 = x^2$, reference model

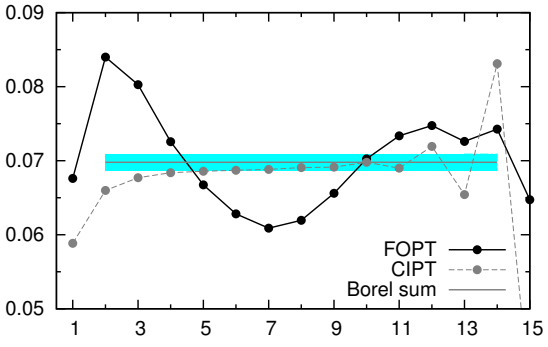

(f) $w_3 = x^2$, alternative model

Figure 1. $\delta^{(0)}_{w_i}$ for $w_1 = 1$, $w_2 = x$, and $w_3 = x^2$, as a function of the order up to which the perturbative series are summed for FOPT (black) and CIPT (gray). The horizontal bands give the Borel resummed result. The left-hand figures are for the RM of ref. [18], the right-hand ones are for the alternative model of eq. (3.9). We use $\alpha_s(m_\tau) = 0.3186$.

behaviour in two parts. In the first terms, the FOPT series again grows rapidly and then decreases. This is a common feature in the other monomials as well. For higher orders, in the RM, FOPT never reaches a plateau: $\delta^{(0)}_{w_2}$ exhibits "run-away" behaviour and decreases monotonically from the 3rd order. The FOPT series shows no sign of stabilisation around the true value, though it develops an inflection point close to the Borel sum. The sign of

JHEP01(2013)125

the run-away behaviour (negative) is correlated with the sign of the x monomial (positive). For the alternative model, FOPT still oscillates around the true value. CIPT, on the other hand, is rather stable until the onset of asymptoticity, and provides a good approximation in both models. The results in this prescription are within the Borel resummed values for the RM, given the larger ambiguity in this case. The larger ambiguity stems from the fact that the moment is maximally sensitive to the gluon condensate contribution. This gives a larger contribution from the ambiguity of the IR singularity at $u = 2$, which is (artificially) absent in the AM.

From this discussion of monomial moments we can already extract a few important observations:

- In the AM CIPT always provides the better approximation. This seems to be a generic feature of the AM, not restricted to the kinematical weight.
- In the reference model, the monomial $w_2 = x$ is problematic for FOPT due to run-away behaviour, which is correlated with the large $d = 4$ condensate contribution to this moment.
- For the other monomials low-order approximations in both FOPT and CIPT are problematic in the RM case. However, while FOPT converges to the Borel sum for $n \gtrsim 5$, CIPT never reaches it. This is similar to the behaviour found in ref. [18] for the kinematical weight.

In the following, we discuss the remaining moments w_6 to w_{17} which are composed of the monomial terms. Their behaviour can essentially be understood as a linear combination of what has been discussed in this section.

4.2 Pinched weights with a "1"

We now turn our attention to moments with pinching and start with moments that contain a term "1" in the weight function and that do not have a linear term x. In table 2, these moments are w_7, w_8, w_τ. For all these moments, the term 1 sets the scale and the higher powers only introduce corrections to this leading result. Since they are pinched moments, they always have at least one negative term. This leads, in general, to a stabilisation of FOPT in both models.

In the case of FOPT for the RM, the monomials in w_τ and w_7 conspire to give an excellent cancellation of the initial overshooting, leading to a series that approaches the Borel sum very fast. The cancellations between $c_n \delta^{\text{tree}}_{w_i}$ and $g_n^{[w_i]}$ then make FOPT rather stable after approaching the true value. This can be observed in the results for the RM given in figures 2(a), 2(c), and 2(e). The results for $w_8 = 1 - x^3$ resemble more the ones for $w_1 = 1$ since the corrections due to x^3 are quite small. CIPT, on the other hand, misses the cancellations and never approaches the Borel resummed values. We also observe that the CIPT series enters the sign alternating regime earlier than FOPT. The corresponding results for the AM are shown in figures 2(b), 2(d), and 2(f). As foreseen, here CIPT tends to give a better approximation to the resummed series. Albeit more stable than in the case of the monomials, FOPT still displays oscillations around the Borel sum.

JHEP01(2013)125

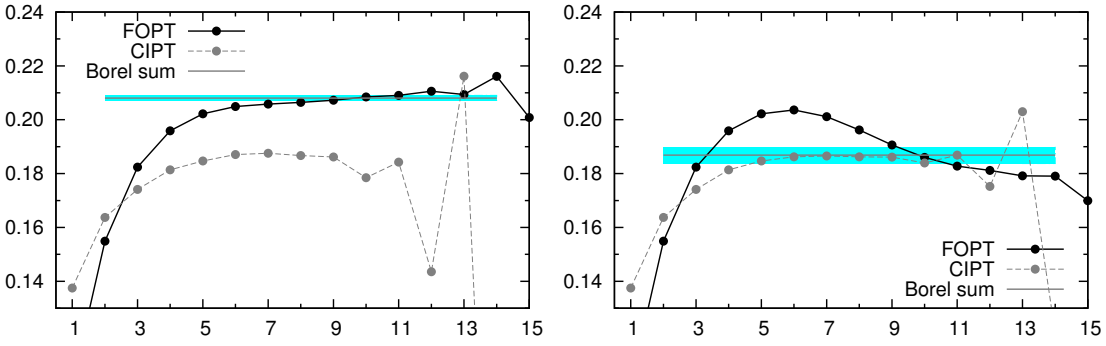

(a) $w_\tau = (1-x)^2(1+2x)$, reference model

(b) $w_\tau = (1-x)^2(1+2x)$, alternative model

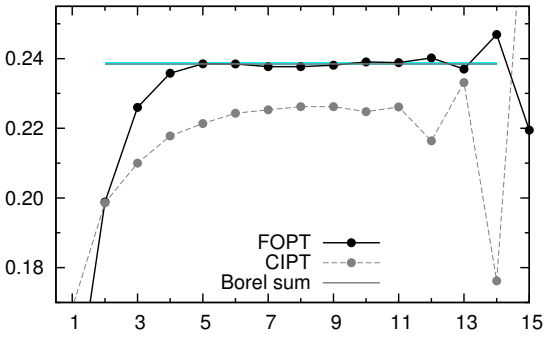

(c) $w_7 = 1-x^2$, reference model

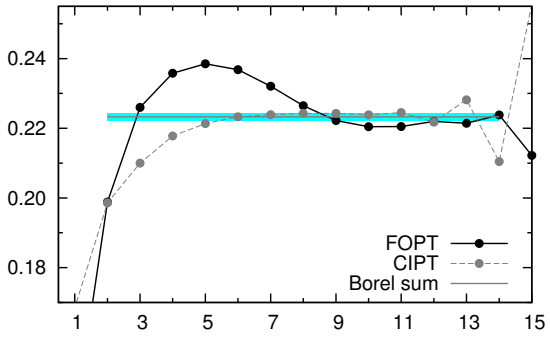

(d) $w_7 = 1-x^2$, alternative model

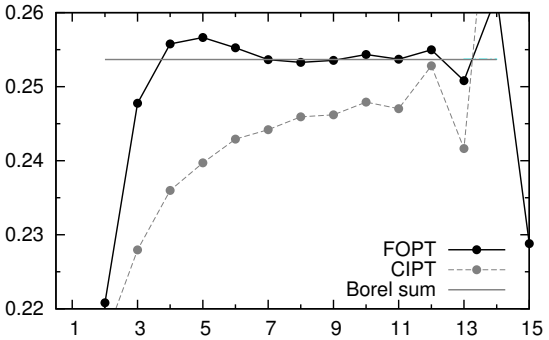

(e) $w_8 = 1-x^3$, reference model

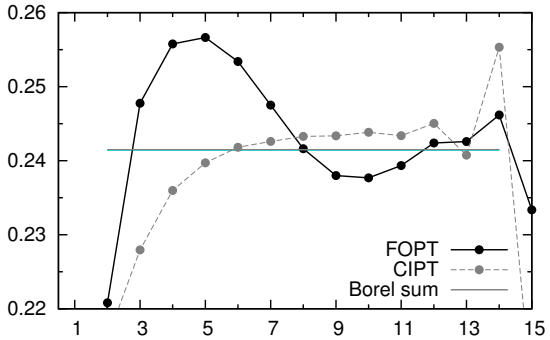

(f) $w_8 = 1-x^3$, alternative model

Figure 2. $\delta^{(0)}_{w_i}$ for w_τ, w_7, and w_8, as a function of the order up to which the perturbative series are summed for FOPT (black) and CIPT (gray). The horizontal bands give the Borel resummed result. The left-hand figures are for the RM of ref. [18], the right-hand ones are for the alternative model of eq. (3.9). We use $\alpha_s(m_\tau) = 0.3186$.

There are many other possible moments, not shown in table 2, that display a very similar behaviour. We have investigated the family $w(x;a) = 1 + ax^2 - (a+1)x^3$ for several different values of a with results rather similar to the ones discussed above. Other moments that do not start with the unity, but with another constant of the same order

JHEP01(2013)125

such as $w(x) = \frac{2}{3}(1-x)^2(1+x)(1+x+4x^2)$ also give qualitatively similar results. Thus, the main observation for this class is that

- pinched-moment weights with a "1" but no linear term all behave similar to the kinematic weight w_τ, favouring FOPT over CIPT for the reference model and vice versa for the alternative model. In each case the perturbative expansion in low orders approaches the Borel sum rather quickly.

4.3 Pinched weights without a "1"

The next class of moments that we analyse here are moments with pinching but that do neither contain a constant term nor one linear in x. As examples for this group we employ w_{16} and w_{17} of table 2; two of the triply-pinched moments used by ALEPH and OPAL [3–6]. In ALEPH's notation, these moments are part of a family denoted by $w^{(1,k)}$, and read

$$w^{(1,k)} \;=\; (1-x)^3 x^k (1+2x) \;=\; x^k - x^{k+1} - 3\,x^{k+2} + 5\,x^{k+3} - 2\,x^{k+4}\,. \tag{4.2}$$

In table 2 we have $w_{13} = w^{(1,0)}$, $w_{15} = w^{(1,1)}$, $w_{16} = w^{(1,2)}$, and $w_{17} = w^{(1,3)}$. Besides the "1" in w_{13}, both the first two also contain a linear term in x and will be discussed in the next section. From table 2 we see that the pinched weights without a "1" have very small $\delta_{w_i}^{\text{tree}}$ but $\mathcal{O}(1)$ coefficients of the monomials. This enhances the relative importance of power corrections.

We consider first the case of w_{16} in the RM, shown in figure 3(a). As expected, $\delta_{w_{16}}^{(0)}$ is tiny, almost 50 times smaller than the corresponding correction for $w_1 = 1$. The combination of powers of x does not improve the behaviour of FOPT that overshoots largely the Borel sum in the first few orders. It eventually approaches the Borel result for higher orders, just before the onset of asymptoticity. The bad behaviour of CIPT already observed for the monomials is amplified and the CIPT series goes astray. The situation in the AM is somewhat improved, but mainly due to the large Borel ambiguity associated with the IR pole at $u = 2$, see figure 3(b). Again, FOPT displays large oscillations around the Borel result, whereas CIPT grows monotonically away from the resummed result before the sign-alternating asymptotic behaviour sets in. As seen in figure 3(c), for FOPT in the RM, the perturbative contribution to the moment of w_{17} has a behaviour qualitatively similar to w_{16}, though for higher orders it is slightly more stable. Also CIPT approaches the Borel sum before the series becomes asymptotic after the 9th order. In the AM, figure 3(d), both, FOPT and CIPT fail to approach the Borel sum, FOPT once more displaying large oscillations.[8] We therefore conclude:

[8] A possible criticism against our analysis of w_{17} within the reference model could regard the lack of an IR singularity at $u = 4$. Since the moment starts with x^3 it is maximally sensitive to $D = 8$ contributions in the OPE, which corresponds to the ambiguity of the IR renormalon at $u = 4$. We investigated this issue by considering a model where one adds an IR renormalon at $u = 4$ and leaves only a constant d_0^{PO} in the model. (This model is briefly discussed on page 24 of ref. [18].) After performing the matching, the residue of the renormalon at $u = 4$ turns out to be small ($d_4^{\text{IR}} = 5.64$) and the changes in the other parameters negligible. The additional Borel ambiguity arising from $u = 4$ is also small. Therefore, the result shown in figure 3(c) is not altered in any significant way, which corroborates the assumption that the singularities at $u = 2$ and $u = 3$ are the dominant ones.

JHEP01(2013)125

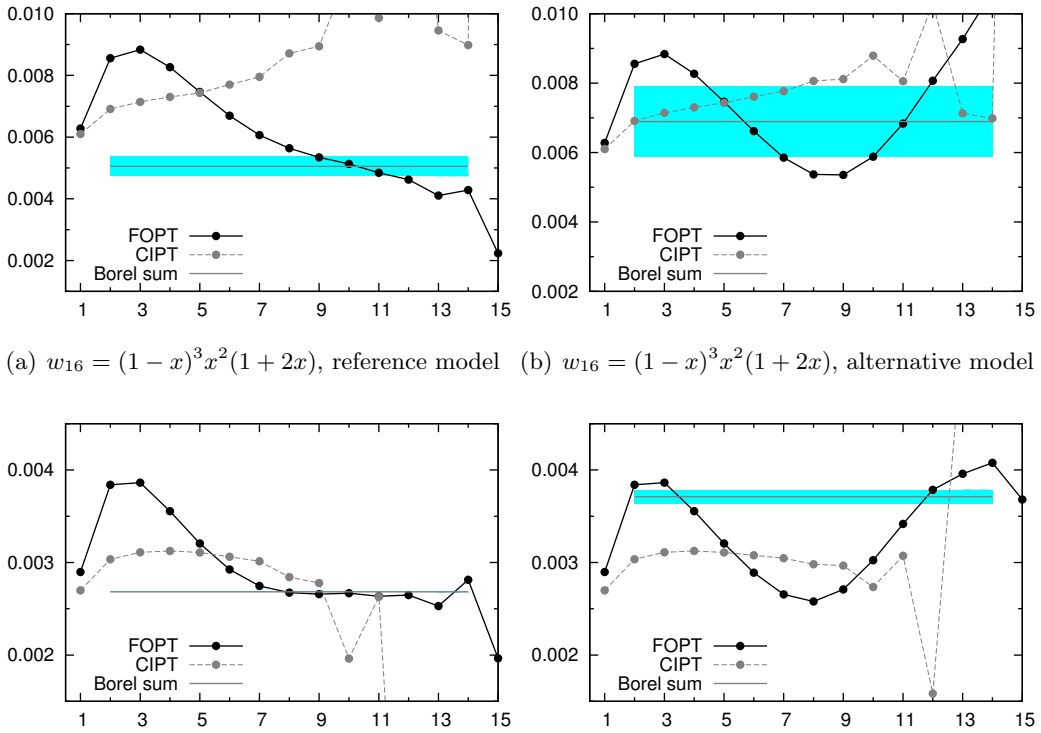

(a) $w_{16} = (1-x)^3x^2(1+2x)$, reference model (b) $w_{16} = (1-x)^3x^2(1+2x)$, alternative model

(c) $w_{17} = (1-x)^3x^3(1+2x)$, reference model (d) $w_{17} = (1-x)^3x^3(1+2x)$, alternative model

Figure 3. $\delta^{(0)}_{w_i}$ for w_{16} and w_{17}, as a function of the order up to which the perturbative series are summed for FOPT (black) and CIPT (gray) are summed. The horizontal bands give the Borel resummed result. The left-hand figures are for the RM of ref. [18], the right-hand ones are for the alternative model of eq. (3.9). We use $\alpha_s(m_\tau) = 0.3186$.

- The perturbative expansions for this class of moments tends to be unreliable in both FOPT and CIPT, and independent of the model for the unknown higher-order coefficients.

- Pinched moments without a "1" are sensitive to condensates, but the poor perturbative approximations render condensate determinations from these moments unreliable. This conclusion appears to be largely model-independent.

4.4 Moments containing a term x

We have relegated to this section the analysis of weight functions containing the monomial x. This choice is based on the observation that the behaviour of these moments, which are maximally sensitive to the $D = 4$ correction in the OPE, is qualitatively different in the RM of ref. [18]. This was shown for the monomial above and here we discuss pinched weights containing this term. There are several of them in table 2: w_6, w_9, w_{10}, w_{11}, w_{13}, w_{14}, and w_{15}. Again, they display very similar qualitative behaviours and it suffices to expose in detail only three representative examples.

JHEP01(2013)125

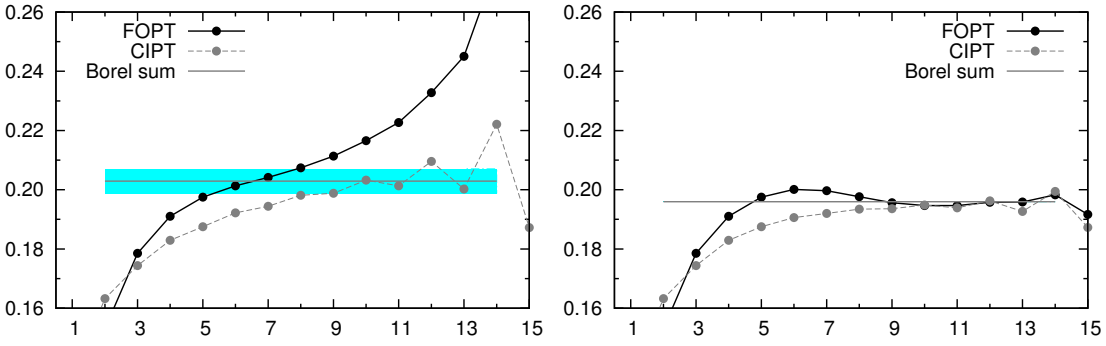

(a) $w_6 = 1 - x$, reference model

(b) $w_6 = 1 - x$, alternative model

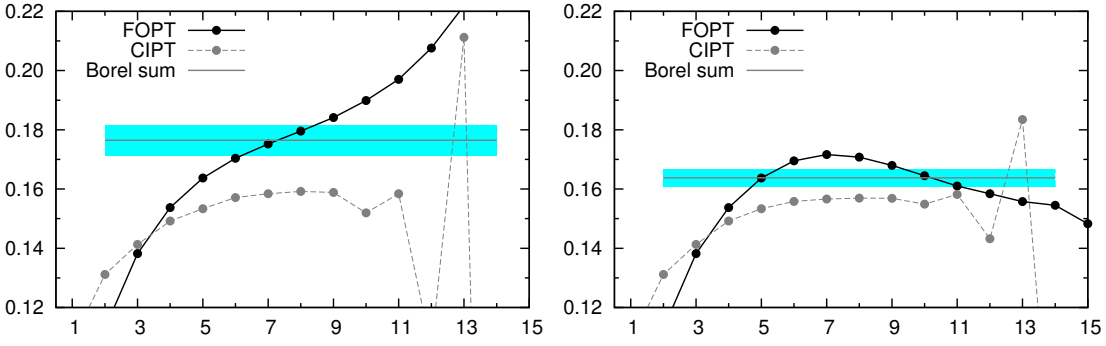

(c) $w_{13} = (1-x)^3(1+2x)$, reference model

(d) $w_{13} = (1-x)^3(1+2x)$, alternative model

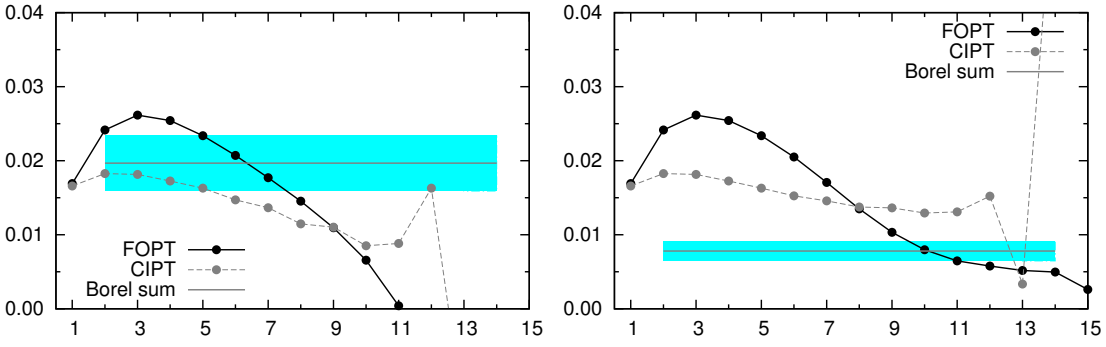

(e) $w_{15} = (1-x)^3x(1+2x)$, reference model

(f) $w_{15} = (1-x)^3x(1+2x)$, alternative model

Figure 4. $\delta^{(0)}_{w_i}$ for w_6, w_{13}, and w_{15}, as a function of the order up to which the perturbative series are summed for FOPT (black) and CIPT (gray). The horizontal bands give the Borel resummed result. The left-hand figures are for the RM of ref. [18], the right-hand ones are for the alternative model of eq. (3.9). We use $\alpha_s(m_\tau) = 0.3186$.

We start with the simple case of $w_6 = 1 - x$, figure 4(a). The term 1 sets the scale, but now, since the perturbative series for the monomial $w_2 = x$ decreases monotonically, the perturbative series for w_6, whose linear coefficient has negative sign, grows monotonically. The result for FOPT crosses the Borel resummed value around the 7th order where it also

JHEP01(2013)125

has an inflection point. CIPT can only approach the Borel sum shortly before it becomes asymptotic around the 9th order. The situation is very similar when higher orders of x are added to the weight function. In figure 4(c), the moment w_{13} is displayed as a representative example. (It corresponds to $w^{(1,0)}$ in ALEPH's notation [3–5] of eq. (4.2)). This weight starts with $1 - x$ followed by higher-order terms in x. Qualitatively, the only difference now is that CIPT never comes close to the Borel sum. The picture changes in the case of w_{15} (or $w^{(1,1)}$) since the term 1 is missing. As figure 4(e) shows, this case is more similar to the monomial x itself, though the higher powers in x soften the behaviour. For CIPT, the situation is not much different either, but it only approximately represents the Borel sum at low orders.

For the alternative model which does not contain the renormalon singularity at $u = 2$, the first two moments w_6 and w_{13}, figures 4(b) and 4(d), are similar to what was observed in the case of pinched moments with the term 1. Now, however, CIPT approaches the Borel results less fast in the case of w_6, and not at all in the case of w_{13}. FOPT in both cases displays oscillations around the true value. The last case, that of w_{15} shown in figure 4(f), is less satisfactory. As was the case for other moments from weight functions starting with a power of x, the values of $\delta^{(0)}_{w_{15}}$ are small. While CIPT misses the Borel sum completely, FOPT only approaches it around the 10th order. We summarise our observations as:

- Weights without a "1" are again unreliable in FOPT and CIPT, and in both models, especially at intermediate orders.
- In the RM, FOPT exhibits run-away behaviour and CIPT may not approach the resummed result. Overall, the perturbative expansion does not behave as well as for moments without a linear term, which is related to the sizeable $D = 4$ power correction.
- In the AM there is no clear preference for one of the two methods.

4.5 Main lessons from the moment analysis

While we already summarised our main observations for each class of weight functions, we collect again here the most important points.

Some of the pinched-moments (with the "1", without the "x") display a particularly fast convergence of FOPT towards the Borel resummed values, especially the moments w_τ and w_7, as shown in figures 2(a) and 2(c). On the contrary, in Borel models that contain a $u = 2$ pole residue of natural size, CIPT generally does not approach the Borel sum before the divergence of the series sets in. This is different in the alternative model, where the $u = 2$ pole is artificially suppressed, and it coincides with the main findings of ref. [18]. Thus, if the reference model is adopted as the most plausible one (as we would do), one again arrives at the conclusion that FOPT provides a better approximation than CIPT, also at order $n = 4, 5$.

The investigation of moments also reveals that the qualitative behaviour of their perturbative expansion depends only on a few features of the moment and the model of the

JHEP01(2013)125

Adler function. As concerns the model, we have already emphasised the crucial question of the size of the residue of the $u = 2$ singularity that corresponds to the $D = 4$ power correction, which motivated the choice of the AM.

As concerns the moment function itself, an important observation is that moments that start with high powers of x, such as w_{15} and w_{16}, employed by the ALEPH and OPAL collaborations, have a bad behaviour of the perturbative series. For these moments, neither FOPT nor CIPT are able to provide a decent approximation to the Borel resummed values in the first few orders. Also, these moments have a very small value of $\delta_{w_i}^{(0)}$, with large relative Borel ambiguities, which makes the reliable separation of power corrections from the uncertain perturbative approximation problematic. Therefore, these moments are not an optimal choice for an α_s analysis. (This has already been pointed out in ref. [7].)

Finally, for moments that contain a linear term x, the reference model, or others that include an IR pole at $u = 2$, both FOPT and CIPT behave badly. In the case of FOPT, the series is quite unstable, which results in large errors due to the truncation of the series, producing unstable results for α_s. (This was noticed — in practice — in the exploratory fits of ref. [40], and it is the reason why, in refs. [8, 9], moments with the term x were not considered.) The situation of CIPT for these moments is also unsatisfactory because the series are unstable and/or do not approach the Borel resummed result. This suggests that moments with a linear term x should also be avoided in α_s determinations.

5 Validation of the reference model

In the previous section we learnt that for moments with good perturbative convergence the comparison of FOPT and CIPT leads to the same conclusion as for the inclusive hadronic tau width studied in ref. [18]. Hence, the crucial factor in deciding whether FOPT or CIPT should be the method of choice remains the plausibility of the reference ansatz for the Adler function (favouring FOPT) as compared to, e.g., the alternative model (favouring CIPT). In addition to the general arguments for the reference model reviewed in section 3, we discuss in this section two further checks, one inspired by ref. [24], which support the plausibility of the ansatz and results of ref. [18].

5.1 Adding a u^2 polynomial term

In ref. [18], the known higher-order coefficients, plus an estimate for $c_{5,1}$, are used to fix the residua of the renormalon poles, while the first two polynomial terms are obtained by also fitting the coefficients $c_{1,1}$ and $c_{2,1}$. It is assumed, therefore, that the renormalons dominate at intermediate (and higher) perturbative orders. However, the fact that $d_1^{\rm PO}$ is small in the reference model of [18], indicates that $c_{2,1}$ is already well saturated by the renormalon poles. The procedure has been criticised in ref. [24], where the authors argue that the truncation of the polynomial terms at linear order is arbitrary. They propose to add a u^2 term to the polynomial and study the behaviour of those models when the coefficient $d_2^{\rm PO}$ is fixed to six different values: $d_2^{\rm PO} = -1, -0.5, 0, 0.25, 0.5, 1$. For the value $d_2^{\rm PO} = 0$, the RM is recovered.

JHEP01(2013)125

	$d_2^{\rm IR}$	$d_3^{\rm IR}$	$d_1^{\rm UV}$	$d_0^{\rm PO}$	$d_1^{\rm PO}$	$d_2^{\rm PO}$ (fixed)
RM [18]	3.16	−13.5	-1.56×10^{-2}	0.78	7.66×10^{-3}	0
$+u^2$ [24]	−1.50	149.7	-5.90×10^{-2}	10.68	3.85	1
$-u^2$ [24]	7.82	−176.8	2.79×10^{-2}	−9.12	−3.83	−1

Table 3. Parameter values of three models for the physical Adler function. "RM" represents the central reference model of ref. [18]. The models denoted by "$\pm u^2$" are those discussed in ref. [24] where the polynomial coefficient $d_2^{\rm PO}$ is taken to be ± 1.

The inclusion of a *fixed* u^2 term in the modelling of the Borel transform of the Adler function has consequences for the residua of the renormalon poles. They have to adjust to the existence of this term which contributes to $c_{3,1}$, which leads to abnormally high values for the residue of the IR pole at $u = 3$, see table 3. Consequently, large cancellations among the contributions of the IR poles at $u = 2$ and $u = 3$ arise. In the two extreme cases studied in [24] , $d_2^{\rm PO} = \pm 1$, the residue of the pole at $u = 3$ changes by factors of -11 and 13 with respect to the RM of [18], for $d_2^{\rm PO} = +1$ and $d_2^{\rm PO} = -1$ respectively. Furthermore, fixing the u^2 term also forces a break-down of the renormalon dominance of the coefficients $c_{2,1}$ and $c_{3,1}$. This is apparent from the values of the other polynomial terms. In the extreme cases $d_2^{\rm PO} = \pm 1$, the module of the coefficient $d_0^{\rm PO}$ is more than 10 times larger than in the RM. The next coefficient, $d_1^{\rm PO}$, is also much larger, more than 100 times the one found in [18]. The values for the residua and the polynomial terms for the RM and for the extreme cases $d_2^{\rm PO} = \pm 1$ are given in table 3. Finally, the coefficient $d_2^{\rm PO}$ and the $u = 2$ residue $d_2^{\rm IR}$ share an almost linear relation, such that $d_2^{\rm IR}$ vanishes for $d_2^{\rm PO} = 0.678$. This particular case constitutes another model for which CIPT generally better approximates the Borel sum for $\delta_{w_i}^{(0)}$.

The inspection of the Adler function $\widehat{D}(s)$ on the complex circle $s = m_\tau^2 {\rm e}^{i\phi}$ sheds further light on the plausibility of the models considered here. It is expected that the perturbative expansion breaks down in the vicinity of the physical, Minkowskian axis ($\phi \sim 0$ or $\phi \sim 2\pi$), but that it should work well in the Euclidean region $\phi \sim \pi$. The behaviour of ${\rm Re}[\widehat{D}(\phi)]$ along the complex contour is displayed in figure 5, of which the upper plot corresponds to FOPT and the lower to CIPT. The dotted, dot-dashed and double-dot-dashed curves are the 3rd, 4th and 5th order purely perturbative results respectively. The thick solid line corresponds to the Borel sum of the reference model. An analogous plot was already shown as figure 9 in appendix B of [18]. In addition, we now also display the additional models with $d_2^{\rm PO} = 1$ (short-dashed line) and $d_2^{\rm PO} = -1$ (long-dashed line). Furthermore, the shaded area indicates the 5th order PT result when the coefficient $c_{5,1}$ is varied in the range $c_{5,1} = 283 \pm 283$.

The following observations can be made on the basis of figure 5. For an asymptotic expansion, the last included term should provide an approximate error estimate for the full sum. Though this is strictly true only for sign-alternating asymptotic series, we expect the estimate not to be wildly violated. Employing the shaded area as such an error estimate, it is seen that in the Euclidean, $\phi \sim \pi$, the RM of [18] lies rather close to this region. On the

JHEP01(2013)125

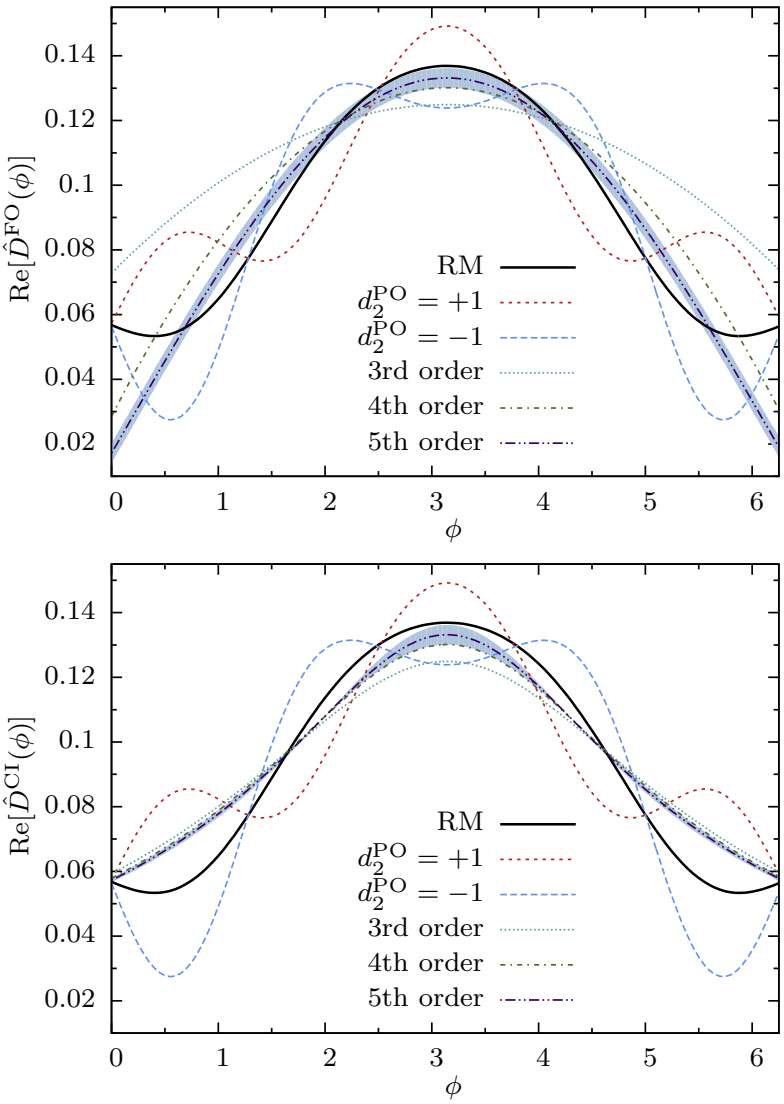

Figure 5. Real part of the Adler function $\widehat{D}(s)$ on the complex circle $s = m_\tau^2 e^{i\phi}$. Borel sums are displayed for the RM (solid line), $d_2^{\mathrm{PO}} = 1$ (short-dashed line) and $d_2^{\mathrm{PO}} = -1$ (long-dashed line). The dotted, dot-dashed and double-dot-dashed lines correspond to 3rd, 4th and 5th order of perturbation theory. Finally, the shaded area indicates the 5th order PT result while varying $c_{5,1} = 283 \pm 283$. The upper plot shows FOPT and the lower CIPT. We employ $\alpha_s(m_\tau) = 0.3186$.

other hand, the models with $d_2^{\mathrm{PO}} = \pm 1$, even in the Euclidean domain where PT should work well, lie far from 5th order perturbation theory. Furthermore, moving away from the Euclidean axis, strong oscillations in $\mathrm{Re}[\widehat{D}(\phi)]$ are found in those models. It seems rather unlikely to us that QCD behaves in this way. Turning the argument around and investigating which values of d_2^{PO} would yield models compatible with the shaded area, we roughly obtain the range $-0.55 < d_2^{\mathrm{PO}} < 0$.

To summarise, there are two arguments in favour of the procedure adopted in ref. [18] for the treatment of the polynomial terms in the ansatz of eq. (3.6). First, the fact that d_1^{PO} turns out to be so small in the central model fit, together with the observed hierarchy

JHEP01(2013)125

$d_0^{\rm PO} \gg d_1^{\rm PO}$, which leads to a renormalon dominance of the coefficients at orders as low as α_s^2. Second, the unnaturalness of the Adler function shape along the circle when $\mathcal{O}(1)$ values of $|d_2^{\rm PO}|$ are imposed in the extended model suggested in ref. [24] that seems to obstruct duality even in the Euclidean region.

5.2 Matching in the large-β_0 limit

Another check whether a simple ansatz such as eq. (3.6) can work can be derived from the large-β_0 limit. As discussed in section 3, an analytic result for the Borel-transformed Adler function is available in this limit, eq. (3.4), and hence the exact perturbative coefficients $c_{n,1}$ are known to all orders [36, 37]. Here, we propose to emulate the matching procedure performed in QCD in the context of the large-β_0 approximation. That is, we make a simple ansatz similar to the RM and fit the parameters of this ansatz to the low-order $c_{n,1}$ in the large-β_0 approximation. We then compare the so-obtained model for the higher-order terms to the exactly known ones.

In order to implement the matching procedure in the case of the large-β_0 limit, we adapt the reference model to the present case by using simple and double poles (instead of branch cuts) for the renormalon singularities. In the spirit of eq. (3.6), the new model can then be written as

$$B[\widehat{D}](u) \,=\, \frac{d_2^{\rm IR}}{2-u} + \frac{d_3^{\rm IR}}{(3-u)^{1+\gamma_3}} + \frac{d_1^{\rm UV}}{(1+u)^2} + d_0^{\rm PO} + d_1^{\rm PO}\,u + d_2^{\rm PO}\,u^2. \tag{5.1}$$

When emulating the procedure of ref. [18], we set the term $d_2^{\rm PO} = 0$. In large-β_0, the IR pole at $u = 3$ is a double pole and therefore $\gamma_3 = 1$. We simulate our ignorance of the structure of this pole in full QCD by taking either $\gamma_3 = 0$ or $\gamma_3 = 1$. From eq. (5.1), by changing γ_3 and the assumptions about $d_2^{\rm PO}$, we define five different models and perform the matching to the first coefficients of the exact large-β_0 Adler function. The models will be denoted by the values of these parameters as $M(\gamma_3; d_2^{\rm PO})$. In the remainder of this section the characteristics of these models are discussed, the matching is described, and we compare with the exact large-β_0 limit.

We begin by performing the matching treating the term $d_2^{\rm PO}$ as suggested in ref. [18], which is equivalent to setting $d_2^{\rm PO} = 0$. Furthermore we employ $\gamma_3 = 1$, which gives a double pole for the IR singularity at $u = 3$, in agreement with the exact result eq. (3.4). This model is referred to as $M(1; 0)$. The renormalon residua are fixed to the coefficients $c_{3,1}$, $c_{4,1}$, and $c_{5,1}$; the two polynomial terms are found by enforcing the true large-β_0 values of $c_{1,1}$ and $c_{2,1}$. The results of this model are shown in the second row of table 4. As in the full QCD case, the value of $d_1^{\rm PO}$ turns out to be small, and significantly smaller then $d_0^{\rm PO}$, indicating the renormalon dominance at intermediate orders. Furthermore, the residua of the renormalon poles are in the ball-park of the true results, although they have to compensate for the lack of higher order poles.

Since the purpose of the model introduced in ref. [18] was to decide upon the best way to perform the RG improvement of the series, it is legitimate to ask if the description of higher orders is successful in the present case. This can now be unambiguously tested by comparing the higher order coefficients predicted by the fitted Adler function with the exact

JHEP01(2013)125

	$d_2^{\rm IR}$	$d_3^{\rm IR}$	$d_1^{\rm UV}$	$d_0^{\rm PO}$	$d_1^{\rm PO}$	$d_2^{\rm PO}$
large-β_0	17.84	−10.49	6.68×10^{-2}	...	...	...
$M(1;0)$	16.53	−45.79	4.10×10^{-2}	−2.90	−0.44	0 (fixed)
$M(0,0)$	8.34	−18.43	4.46×10^{-2}	2.25	0.27	0 (fixed)
$M(1;\text{free})$	18.85	−55.02	3.92×10^{-2}	−3.03	−0.34	5.79×10^{-2}
$M(1,1)$	56.54	−205.27	9.76×10^{-3}	−5.15	1.31	1 (fixed)
$M(1,-1)$	−23.46	113.67	7.23×10^{-2}	-6.52×10^{-1}	−2.19	−1 (fixed)

Table 4. Residues of poles and polynomial parameters of the models discussed in the text. The first row gives the exact result in the large-β_0 approximation. The models are defined by the values of γ_3 and $d_2^{\rm PO}$ in eq. (5.1) and denoted by $M(\gamma_3; d_2^{\rm PO})$.

	$c_{6,1}$	$c_{7,1}$	$c_{8,1}$	$c_{9,1}$	$c_{10,1}$	$c_{11,1}$
large-β_0	-1.99×10^3	9.86×10^4	-1.08×10^6	2.78×10^7	-5.39×10^8	1.40×10^{10}
$M(1;0)$	-2.46×10^3	1.08×10^5	-1.30×10^6	3.28×10^7	-6.68×10^8	1.74×10^{10}
$M(0;0)$	-3.53×10^3	1.08×10^5	-1.51×10^6	3.46×10^7	-7.38×10^8	1.87×10^{10}
$M(1;\text{free})$	input	1.07×10^5	-1.21×10^6	3.17×10^7	-6.35×10^8	1.67×10^{10}
$M(1;1)$	5.69×10^3	8.54×10^4	2.74×10^5	1.39×10^7	-9.09×10^7	4.95×10^9
$M(1;-1)$	-1.06×10^4	1.30×10^5	-2.88×10^6	5.17×10^7	-1.25×10^9	2.98×10^{10}

Table 5. Higher-order coefficients from the five models described in the text compared with the exact large-β_0 results. Models are defined by the values of γ_3 and $d_2^{\rm PO}$ in eq. (5.1) as $M(\gamma_3; d_2^{\rm PO})$.

results in large-β_0. Numerically, this comparison is shown in table 5. Graphically, FOPT, CIPT, and the resummed results for the model are shown in figure 6(b) (for w_τ), whereas the equivalent plot for the exact large-β_0 results is given in figure 6(a). The qualitative agreement of the results of table 5, together with the striking similarities of figures 6(a) and 6(b), demonstrate that — in spite of the simplifications of the model with respect to the exact results — the model reproduces faithfully the FOPT and CIPT series up to higher orders, as well as the Borel resummed value.

In the previous model, the parameter γ_3 was fixed to the true value of the large-β_0 limit. Let us investigate the consequences of a wrong choice for γ_3. For full QCD this is a relevant open issue as several operators contribute at $D = 6$, and the general renormalon structure has not yet been established. We define a new model that differs from the previous one only by having a simple pole at $u = 3$, thus $\gamma_3 = 0$. Accordingly, we denote this model by $M(0;0)$. Performing the matching, we find the results of the 3rd row of table 4. The choice $\gamma_3 = 0$ enforces a number of adjustments in the parameters of the model with respect to the case where $\gamma_3 = 1$. The residue of the pole at $u = 2$ changes and is less well reproduced than in the previous case. The polynomial terms are different, but the hierarchy between the terms is still preserved. In particular, inspection of the third row of table 5, together

JHEP01(2013)125

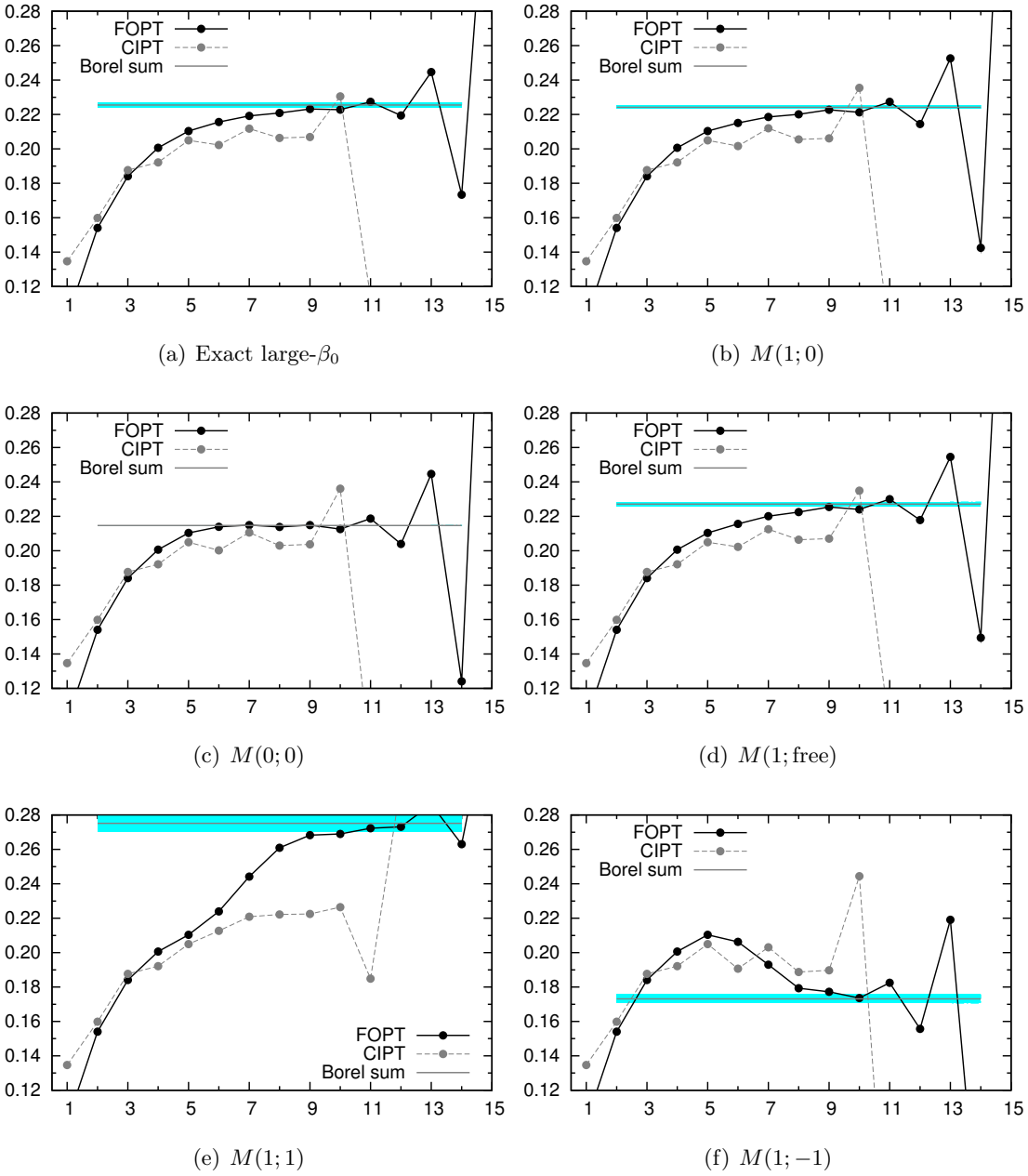

(a) Exact large-β_0 (b) $M(1;0)$

(c) $M(0;0)$ (d) $M(1;\text{free})$

(e) $M(1;1)$ (f) $M(1;-1)$

Figure 6. Values of $\delta_{w_\tau}^{(0)}(m_\tau^2)$ as a function of the order n up to which the perturbative series has been summed for FOPT (black) and CIPT (gray). Horizontal gray lines give the Borel resummed result and the bands give the estimated ambiguity. In (a) one sees the result from the exact large-β_0 limit. In (b)-(f), we show results from models matched to the first few coefficients of the large-β_0 Adler function (see text). Models are defined by the values of γ_3 and $d_2^{\rm PO}$ in eq. (5.1) as $M(\gamma_3; d_2^{\rm PO})$. For consistency with large-β_0, we perform the α_s running at one loop. We use $\alpha_s(m_\tau^2) = 0.3186$.

with figure 6(c) shows that the higher-order behaviour of FOPT and CIPT continues to resemble very much the exact result. In agreement with figure 6(a), FOPT approaches the Borel resummed value better than CIPT. Still, one must admit that there is a shift

JHEP01(2013)125

in the Borel resummed value of $\sim 5\%$, which is beyond the ambiguity of the exact result ($\sim 1\%$). Nevertheless, the conclusions about FOPT versus CIPT — and the superiority of the former — remain intact.

We now investigate the question of adding a term $d_2^{\rm PO} u^2$ in eq. (5.1). Since all coefficients $c_{n,1}$ of the Adler function are available in the large-β_0 approximation, we have the freedom to include the coefficient $c_{6,1}$ in the matching. This allows us to keep the six parameters of the model free, including $d_2^{\rm PO}$, and then follow a strategy similar to the one above (we use $\gamma_3 = 1$). This model is termed $M(1;\text{free})$. We employ the coefficients $c_{4,1}$, $c_{5,1}$, and $c_{6,1}$ to fix the residua of the renormalon poles, while the polynomial terms are fixed by $c_{3,1}$, $c_{2,1}$, and $c_{1,1}$. The results after matching are found in the third row of table 4. The inclusion of the free parameter $d_2^{\rm PO}$ preserves the hierarchy $d_0^{\rm PO} \gg d_1^{\rm PO} \gg d_2^{\rm PO}$, indicating the renormalon dominance at intermediate and higher orders. This is in agreement with what was found before, where we kept $d_2^{\rm PO} = 0$ fixed. Table 5 and Fig 6(d) show that the quality of the description of higher orders remains impressive when we introduce the term $d_2^{\rm PO}$ keeping it free and using the procedure of ref. [18] to fix it.

Let us turn now to the consequences of having a fixed parameter $d_2^{\rm PO}$. To make contact with ref. [24], we study the two cases $d_2^{\rm PO} \pm 1$ (again $\gamma_3 = 1$). These configurations are denoted $M(1,\pm 1)$. In table 4, one sees some issues that emanate from this choice. The hierarchy of the polynomial terms is broken and, what is more, the values of the residua of the IR renormalon poles are very different from the exact ones. We observe large values of the residua, leading to strong cancellations between the contributions of the different IR poles, a feature that was already observed in full QCD. What is then the most faithful description of the higher orders? Table 5 demonstrates that the description with fixed $d_2^{\rm PO} \sim \mathcal{O}(1)$ is very poor. The large-order coefficients are badly reproduced; even the sign is wrong in two of them. figures 6(e) and 6(f) show that the perturbative series goes astray, and the Borel resummed results are very different from the exact one shown in figure 6(a).

This exercise shows that the model is incompatible with a u^2 term whose coefficient is of order unity. In real QCD, only four coefficients of the Adler function are known exactly. In such a scenario, it seems that the best strategy is to keep $d_2^{\rm PO} = 0$, since we learn in large-β_0 that fixing this parameter to an arbitrary value is not a better option. A final comment is in order. Figure 6 shows results for the kinematic moment w_τ only. We have studied all moments displayed in table 2 also for large-β_0 and the conclusions regarding the quality of the description are not altered in other cases.

6 Consequences for the determination of α_s

Based on the perturbative behaviour of the Adler function under two different assumptions for the higher-order coefficients, we argued in section 4 that some weight functions are more suitable for an α_s analysis from hadronic τ decays than others. The aim of this section is to corroborate these findings comparing the predicted moments with experimental values. We want to check the internal consistency of the predictions from different moments and study the uncertainties associated with them once all the contributions are taken into account (power corrections and duality violations). Rather than comparing moment predictions

JHEP01(2013)125

with data for some given value of α_s, we perform this consistency check by determining the values of α_s from each individual moment. The spread of α_s values and uncertainties then provides the desired information. We emphasize that the aim of this exercise is *not* a precise determination of the strong coupling.

We consider FESRs for the weight-functions of table 2. In the notation introduced in eq. (2.6), we study the moments $R^{w_i}_{V+A}(m_\tau^2)$, relying on external input for the power corrections and for DVs. A more comprehensive analysis should include more than one moment and treat consistently all the ingredients of the theoretical description: the perturbative series, power corrections, and duality violations. In such an analysis, an involved non-linear multi-parameter fit taking into account all correlations is unavoidable (see e.g. [8, 9]). Here our error bars in α_s are smaller than the ones of a self-consistent analysis due to the fact that we do not perform a multi-parameter fit.

The different theoretical components in the computation of the moments are treated as follows. As discussed in section 2, the perturbative FO and CI series are summed up to order α_s^5 using $c_{5,1} = 283$. The uncertainty due to the truncation of the series is estimated by either taking $c_{5,1} = 0$ or $c_{5,1} = 566$. A third α_s value is obtained from the Borel resummed results of the reference model.

The power corrections in the OPE are taken as an external input. Corrections due to dimension 4, 6, and 8 are considered. (The mass corrections, $D = 2$, are also taken into account although they can safely be neglected due to the smallness of the quark masses.) For $D = 4$, we use the gluon condensate value $\langle aG^2\rangle = (0.012 \pm 0.012)\,\text{GeV}^4$, and include in the coefficient function the known α_s corrections with their logarithms [41]. At dimenstion six, the main contributions arise from the four-quark condensates, since the coefficient of the three-gluon condensate vanishes at leading order and all terms proportional to quark masses can safely be neglected. One usually resorts to the vacuum saturation approximation to write these contributions in terms of squares of the quark condensate [44], introducing the parameter ρ_{V+A} to account for deviations from this assumption. The $D = 6$ corrections are then proportional to $\rho_{V+A}\langle\bar{q}q\rangle^2$. In our estimates we use $\rho_{V+A} = 2 \pm 1$ [18] and $\langle\bar{q}q\rangle(m_\tau) = -(272 \pm 15\ \text{MeV})^3$ [45]. A crude estimate of $D = 8$ is included adding the a term $C_{8,V+A}/s^4$ to the Adler function. To evaluate the impact of this contribution we use $C_{8,V+A} = (0 \pm 5) \cdot 10^{-3}$. Our estimates for $D = 6$ and 8 agree, within uncertainties, with the results of the fits of ref. [9].

A phenomenological estimate of the longitudinal contribution from scalar and pseudoscalar correlators is included in the spirit of refs. [42, 43]. The weight-function dependence of the non-perturbative corrections make some of the moments quite insensitive to the details of the non-perturbative contributions. However, for other weight-functions, this is not the case and the final α_s values depend heavily on the non-perturbative input.

Finally, the contribution from DVs to the moments is computed using the results of ref. [9]. The corresponding term takes the form

$$\delta^{\text{DV}}_{w_i,V/A}(s_0) \;=\; -\,8\pi^2 \int_{s_0}^{\infty} \frac{ds}{s_0}\, w_i(s)\, \rho^{\text{DV}}_{V/A}(s)\,, \tag{6.1}$$

JHEP01(2013)125

where the DV part of the spectral functions, $\rho^{\rm DV}_{V/A}(s)$, is parametrised as [15]

$$\rho^{\rm DV}_{V/A}(s) \,=\, \exp\left(-\delta_{V/A} - \gamma_{V/A} s\right) \sin\left(\alpha_{V/A} + \beta_{V/A} s\right) \,. \tag{6.2}$$

The eight parameters for the description of DVs are taken from the results of a fit to V and A using updated OPAL data shown in table V of ref. [9] (we take the FOPT fit with $s_{\rm min} = 1.5\,{\rm GeV}^2$). Their correlations are employed in the Monte Carlo estimate of the error induced by DVs. Note, however, that within our simplified α_s determination in which DVs and power corrections are not determined self-consistently, the precise DV parameters are not important for the following. Within other errors, the DV term (6.1) has a negligible impact on α_s from the moments discussed below.

The experimental counterparts of the moments $R^{w_i}_{V+A}(m_\tau^2)$ are obtained performing a discretised version of the integral given in eq. (2.2), where the spectral functions are the ones from the ALEPH collaboration after the 2008 update performed in ref. [5]. It is known that in this data set contributions to the correlations due to the unfolding procedure were inadvertently omitted [40]. At present, in a precise determination of α_s, the safest option is to turn to an updated version of the OPAL data [6, 9]. Nevertheless, for our exploratory purposes, this omission is harmless and would only alter the experimental error bars, that are potentially underestimated.

In figure 7, we display results of this simplified α_s analysis for 13 of the weight functions of table 2, and using FOPT, CIPT, and the Borel sum within the RM. (We do not show results for the monomials w_2 to w_5.) The inner error bars give the experimental errors, while the external error bars include the theoretical error as well. The relative size of the experimental uncertainties depends strongly on the moment considered. This is understandable since the spectral functions have larger relative uncertainties in the higher-energy part. Moments that emphasise this region (or that do not suppress it) such as $w_1(x) = 1$ are penalised and have significantly larger uncertainties. In general, pinched moments suppress the edge of the spectrum and have smaller relative uncertainties.

We consider several sources of theoretical errors in α_s. The first one is the truncation of perturbation theory, which is estimated by varying the coefficient $c_{5,1} = 283 \pm 283$. Another source of theoretical error is the residual renormalisation-scale dependence. To estimate this uncertainty, we re-express the FO series in terms of a different scale μ^2, rather than using $a(m_\tau^2)$, and vary this scale. The residual dependence is estimated in CIPT in a similar fashion by setting the scale to $\mu^2 = -\xi^2 s_0 x$ in eq. (2.12). This generates additional logarithms that must be taken into account in $\delta^{(0)}_{{\rm CI},w_i}$. In the Borel resummed model, this scale/model uncertainty is also estimated by taking $\mu^2 = \xi^2 m_\tau^2$, determining $a(\xi m_\tau)$, and evolving the result back to $\mu = m_\tau$. In all cases, the scale is varied in the interval $0.5\, m_\tau^2 \le \mu^2 \le 1.5\, m_\tau^2$. The uncertainty due to $D = 4$ contributions is estimated varying the gluon condensate in the interval $\langle aG^2\rangle = (0.012 \pm 0.012)\,{\rm GeV}^4$. Uncertainties from $D = 6$ and $D = 8$ are computed from the propagation of the error on the quantities ρ_{V+A}, $\langle\bar{q}q\rangle$, and $C_{8,V+A}$. Finally, the uncertainty due to the DV term is estimated from a Monte Carlo sample of parameters generated according to the results found in table V of ref. [9]. The outer error bars in figure 7 contain the sum in quadrature of all these errors together with the experimental uncertainty.

JHEP01(2013)125

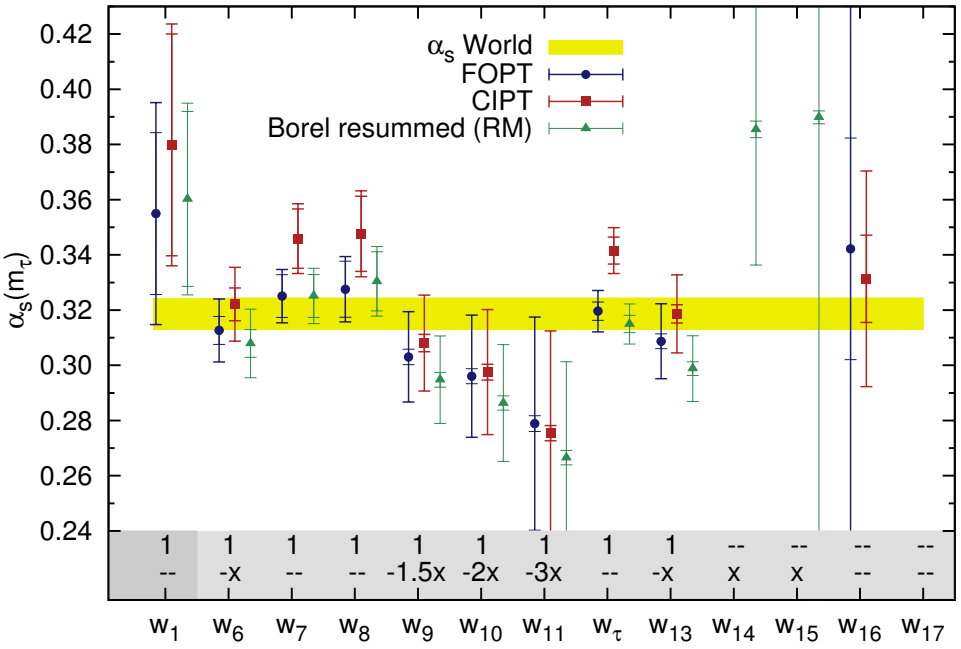

Figure 7. Results of $\alpha_s(m_\tau)$ from $V+A$ sum rules constructed with the weight functions of table 2 and using the 2008 version of ALEPH data [5]. The absence of a point means that no reasonable value of α_s was found. Inner error bars give solely the experimental error; outer bars include the theory error as well. In the lower shaded band we show explicitly the constant term and the term proportional to x for the weight functions (when present). All the moments are pinched except for w_1. The world average of α_s is that of the PDG [46]: $\alpha_s(m_\tau) = 0.3186 \pm 0.0056$.

Let us turn now to an analysis of the results shown in figure 7. A first important point is that for the moments considered ideal in the study of $\delta^{(0)}_{w_i}$, namely, w_7, w_8, and w_τ, we obtain an α_s value compatible with the world average within our simplified analysis. The results from FOPT and the reference model are particularly close to the world average, while CIPT lies about two sigma away. This is a consequence of the fact that $\delta^{(0)}_{w_i}$ dominates these moments, and the FOPT perturbative series shows a good behaviour. They are quite insensitive to the the power corrections and DVs and, accordingly, have relatively small theoretical uncertainties. Their experimental uncertainties are smaller than in other moments due to the suppression of the edge of the spectral functions.

The situation is radically different for w_{14}, w_{15}, and w_{17} for which neither FOPT nor CIPT were able to give a reasonable value of α_s. The Borel resummed result from the reference model of ref. [18] does not yield any acceptable value for α_s for w_{16} and w_{17} either. For w_{14} and w_{15} abnormally high values with huge uncertainties are obtained. This is a manifestation of the bad convergence properties observed for the family of moments $w^{(1,k)}$, defined in eq. (4.2) and used e.g. in refs. [3–6], combined with the fact that these moments receive very large contributions from power corrections (of the order of 50% for w_{17}). Note that with the present treatment of power corrections the theoretical error of these moments is by far dominated by perturbative (scale and $c_{5,1}$ variations) uncertainties. This corroborates the conclusion of section 4, namely, that these moments are not the

JHEP01(2013)125

optimal choice for an α_s analysis from τ decays. For w_{16}, FOPT and CIPT yield a value of α_s with large errors dominated by power corrections of dimension 6 and 8 with a sizeable contribution from the perturbative series. The result in FOPT is particularly unstable, leading to larger uncertainties.

The scenario for the moments that contain an x term and the unity lies in between the previous two. Moments like w_6 and also w_{13} still yield reasonable values of α_s. On the other hand, moments like w_9, w_{10}, w_{11} give lower values of α_s. This can be understood since for these moments the $D = 4$ correction is increasingly important, due to the higher coefficients of the x term. In our estimate, these $D = 4$ corrections are positive which leads to lower values of α_s. This is not the case in w_{13} due to the $D = 6$ and $D = 8$ contributions arising from the terms $-3x^2 + 5x^3$ in the weight function, that compensate the $D = 4$ corrections. Since these moments are more sensitive to $D = 4$, they exhibit larger theoretical uncertainties arising predominantly from $\delta^{(4)}_{w_i,V/A}$.

Finally, from $w_1 = 1$, a value of α_s compatible with the world average is also obtained. This moment has a much larger experimental uncertainty due to the lack of pinching and the corresponding higher contribution from the edge of the spectrum.

A general observation is that the size of the discrepancy between FO and CI also depends strongly on the moment. Moments such as w_9, w_{10}, and w_{11} tend to minimise the discrepancy while the kinematical moment w_τ, and to some extent $w_7 = 1 - x^2$ and $w_8 = 1 - x^3$, tend to maximise this difference. We have seen that FOPT is a better approximation to the Borel resummed results in the reference model; therefore, α_s values from FOPT are systematically closer to the Borel resummed ones than CIPT values.

7 Conclusions

In the first part of this work, we have analysed the moment dependent features of the perturbative expansion of the Adler function needed in the theoretical description of hadronic τ decays. A systematic study of this moment dependence is important since it serves as a guide for future analyses of α_s, and provides further insight on the question whether FOPT or CIPT is a better framework for α_s extractions. To analyse the higher order behaviour of the series we employed two models. The first is the reference model of ref. [18], which gives — we believe — a plausible representation of the QCD Adler function. In this model, FOPT is the prescription that gives the best approximation to the Borel resummed results. In order to assess possible model dependencies in our conclusions, we have also employed a model where the IR pole at $u = 2$, which is the most important one for the perturbative behaviour in intermediate orders, is artificially suppressed; this description favours CIPT. The behaviour of $\delta^{(0)}_{w_i}$ for a large collection of moments can then be divided into a small number of classes. The general behaviour of the perturbative series can be traced back to the singularities of the Borel transformed Adler function and to simple features of the weight-functions.

We have shown that some moments have better perturbative properties than others. Our conclusions are based on the inspection of the perturbative series and on a simplified α_s extraction from each one of the moments. In particular, polynomial pinched weight-

JHEP01(2013)125

functions that contain the unity and do not contain a term proportional to x are found to be optimal. This is due to the good behaviour of the perturbative series in these cases, where at least one of the methods, FOPT or CIPT, provides a good approximation to the Borel resummed results. Another positive feature of these moments is the small contamination by power corrections and DVs. We have shown that some of the moments used in the literature, such as the family of moments $w^{(1,k)}$ [see eq. (4.2)], employed e.g. by ALEPH and OPAL [3, 5, 6], are perturbatively unstable and do not provide good approximations to the Borel resummed results of the models investigated. In the best of the cases, FOPT is capable of approaching the Borel results only at higher orders that are not available in the real QCD case. In addition, the ambiguity introduced by the power corrections is of the same order as the perturbative contribution, rendering the extraction of α_s and condensates from these moments unreliable (similar observations were made in ref. [7]). Moments that contain an x term lie in between the two latter groups. In the reference model, where the contribution of the leading IR pole is significant, they display run-away behaviour in the perturbative series, which engenders larger uncertainties and potential instabilities in α_s results. The contribution from $D = 4$ in the OPE can also be quite sizeable depending on the coefficient of the x term in the weight function. This makes the use of these moments for determinations of α_s and condensates somewhat problematic, although the evidence against their use is less compelling than in the case of moments with only higher powers of x.

Overall, regarding the FOPT/CIPT comparison, the moment analysis confirms the conclusions drawn from the inclusive tau hadronic width [18] in the following sense: whenever perturbatively well-behaved moments are considered, FOPT shows better behaviour in the reference model that is believed to incorporate the main known features of large-order behaviour in QCD. CIPT underestimates the resummed value and therefore leads to systematically larger α_s values.

In section 5, we have provided further evidence to the plausibility of the reference model suggested in ref. [18]. The matching procedure with the first two terms of a polynomial in u in eq. (3.6) was justified based on the behaviour of the Adler function on the complex plane and on comparisons with the large-β_0 limit. This limit provides a laboratory for renormalon models, since the exact result to all orders is known. We have shown that models containing solely the leading singularities capture the general features of the exact result surprisingly accurately. What is more, the use of these models is sufficient to decide upon the best prescription for the RG improvement of the perturbative series. It therefore appears that the reference model is solid and survives criticisms raised in the literature.

Acknowledgments

MB is supported in part by the Gottfried Wilhelm Leibniz programme of the *Deutsche Forschungsgemeinschaft* (DFG). The work of DB is supported by the Alexander von Humboldt Foundation. MJ is partially supported by CICYTFEDER-FPA2008-01430, FPA2011-25948, SGR2009-894, and the Spanish Consolider-Ingenio 2010 Program CPAN (CSD2007-00042).

JHEP01(2013)125

References

[1] Heavy Flavor Averaging Group collaboration, Y. Amhis et al., *Averages of b-hadron, c-hadron and tau-lepton properties as of early 2012*, arXiv:1207.1158 [INSPIRE].

[2] E. Braaten, S. Narison and A. Pich, *QCD analysis of the tau hadronic width*, *Nucl. Phys.* **B 373** (1992) 581 [INSPIRE].

[3] ALEPH collaboration, R. Barate et al., *Measurement of the spectral functions of axial-vector hadronic τ decays and determination of $\alpha_s(M_\tau^2)$*, *Eur. Phys. J.* **C 4** (1998) 409 [INSPIRE].

[4] ALEPH collaboration, S. Schael et al., *Branching ratios and spectral functions of τ decays: final ALEPH measurements and physics implications*, *Phys. Rept.* **421** (2005) 191 [hep-ex/0506072] [INSPIRE].

[5] M. Davier, S. Descotes-Genon, A. Höcker, B. Malaescu and Z. Zhang, *The determination of α_s from τ decays revisited*, *Eur. Phys. J.* **C 56** (2008) 305 [arXiv:0803.0979] [INSPIRE].

[6] OPAL collaboration, K. Ackerstaff et al., *Measurement of the strong coupling constant α_s and the vector and axial vector spectral functions in hadronic tau decays*, *Eur. Phys. J.* **C 7** (1999) 571 [hep-ex/9808019] [INSPIRE].

[7] K. Maltman and T. Yavin, *$\alpha_s(M_Z^2)$ from hadronic tau decays*, *Phys. Rev.* **D 78** (2008) 094020 [arXiv:0807.0650] [INSPIRE].

[8] D. Boito et al., *A new determination of α_s from hadronic τ decays*, *Phys. Rev.* **D 84** (2011) 113006 [arXiv:1110.1127] [INSPIRE].

[9] D. Boito et al., *An updated determination of α_s from τ decays*, *Phys. Rev.* **D 85** (2012) 093015 [arXiv:1203.3146] [INSPIRE].

[10] B. Blok, M.A. Shifman and D.-X. Zhang, *An Illustrative example of how quark hadron duality might work*, *Phys. Rev.* **D 57** (1998) 2691 [*Erratum ibid.* **D 59** (1999) 019901] [hep-ph/9709333] [INSPIRE].

[11] I.I. Bigi, M.A. Shifman, N. Uraltsev and A.I. Vainshtein, *Heavy flavor decays, OPE and duality in two-dimensional 't Hooft model*, *Phys. Rev.* **D 59** (1999) 054011 [hep-ph/9805241] [INSPIRE].

[12] M.A. Shifman, *Quark hadron duality*, hep-ph/0009131 [INSPIRE].

[13] O. Catà, M. Golterman and S. Peris, *Duality violations and spectral sum rules*, *JHEP* **08** (2005) 076 [hep-ph/0506004] [INSPIRE].

[14] O. Catà, M. Golterman and S. Peris, *Unraveling duality violations in hadronic τ decays*, *Phys. Rev.* **D 77** (2008) 093006 [arXiv:0803.0246] [INSPIRE].

[15] O. Catà, M. Golterman and S. Peris, *Possible duality violations in τ decay and their impact on the determination of α_s*, *Phys. Rev.* **D 79** (2009) 053002 [arXiv:0812.2285] [INSPIRE].

[16] M. Jamin, *What two models may teach us about duality violations in QCD*, *JHEP* **09** (2011) 141 [arXiv:1103.2718] [INSPIRE].

[17] M. Jamin, *Contour-improved versus fixed-order perturbation theory in hadronic τ decays*, *JHEP* **09** (2005) 058 [hep-ph/0509001] [INSPIRE].

[18] M. Beneke and M. Jamin, *α_s and the τ hadronic width: fixed-order, contour-improved and higher-order perturbation theory*, *JHEP* **09** (2008) 044 [arXiv:0806.3156] [INSPIRE].

JHEP01(2013)125

[19] A. Pivovarov, *Renormalization group analysis of the tau lepton decay within QCD*, *Z. Phys.* **C 53** (1992) 461 [*Sov. J. Nucl. Phys.* **54** (1991) 676] [*Yad. Fiz.* **54** (1991) 1114] [hep-ph/0302003] [INSPIRE].

[20] F. Le Diberder and A. Pich, *Testing QCD with τ decays*, *Phys. Lett.* **B 289** (1992) 165 [INSPIRE].

[21] P.A. Baikov, K.G. Chetyrkin and J.H. Kühn, *Order α_s^4 QCD corrections to Z and τ decays*, *Phys. Rev. Lett.* **101** (2008) 012002 [arXiv:0801.1821] [INSPIRE].

[22] S. Menke, *On the determination of α_s from hadronic tau decays with contour-improved, fixed order and renormalon-chain perturbation theory*, arXiv:0904.1796 [INSPIRE].

[23] I. Caprini and J. Fischer, *α_s from tau decays: Contour-improved versus fixed-order summation in a new QCD perturbation expansion*, *Eur. Phys. J.* **C 64** (2009) 35 [arXiv:0906.5211] [INSPIRE].

[24] S. Descotes-Genon and B. Malaescu, *A note on renormalon models for the determination of $\alpha_s(M_\tau)$*, arXiv:1002.2968 [INSPIRE].

[25] G. Cvetič, M. Loewe, C. Martinez and C. Valenzuela, *Modified contour-improved perturbation theory*, *Phys. Rev.* **D 82** (2010) 093007 [arXiv:1005.4444] [INSPIRE].

[26] G. Abbas, B. Ananthanarayan and I. Caprini, *Determination of $\alpha_s(M_\tau^2)$ from improved fixed order perturbation theory*, *Phys. Rev.* **D 85** (2012) 094018 [arXiv:1202.2672] [INSPIRE].

[27] W. Marciano and A. Sirlin, *Electroweak radiative corrections to τ decay*, *Phys. Rev. Lett.* **61** (1988) 1815 [INSPIRE].

[28] E. Braaten and C.-S. Li, *Electroweak radiative corrections to the semihadronic decay rate of the τ lepton*, *Phys. Rev.* **D 42** (1990) 3888 [INSPIRE].

[29] J. Erler, *Electroweak radiative corrections to semileptonic tau decays*, *Rev. Mex. Fis.* **50** (2004) 200 [hep-ph/0211345] [INSPIRE].

[30] I.S. Towner and J.C. Hardy, *The evaluation of V_{ud} and its impact on the unitarity of the Cabibbo-Kobayashi-Maskawa quark-mixing matrix*, *Rept. Prog. Phys.* **73** (2010) 046301 [INSPIRE].

[31] S. Gorishnii, A. Kataev and S. Larin, *The $O(\alpha_s^3)$ corrections to $\sigma_{\rm tot}(e^+e^- \to hadrons)$ and $\Gamma(\tau^- \to \nu_\tau + hadrons)$ in QCD*, *Phys. Lett.* **B 259** (1991) 144 [INSPIRE].

[32] L.R. Surguladze and M.A. Samuel, *Total hadronic cross-section in e^+e^- annihilation at the four loop level of perturbative QCD*, *Phys. Rev. Lett.* **66** (1991) 560 [*Erratum ibid.* **66** (1991) 2416] [INSPIRE].

[33] M. Beneke, *Renormalons*, *Phys. Rept.* **317** (1999) 1 [hep-ph/9807443] [INSPIRE].

[34] P. Ball, M. Beneke and V.M. Braun, *Resummation of $(\beta_0\alpha_s)^n$ corrections in QCD: techniques and applications to the tau hadronic width and the heavy quark pole mass*, *Nucl. Phys.* **B 452** (1995) 563 [hep-ph/9502300] [INSPIRE].

[35] M. Neubert, *QCD analysis of hadronic tau decays revisited*, *Nucl. Phys.* **B 463** (1996) 511 [hep-ph/9509432] [INSPIRE].

[36] M. Beneke, *Large order perturbation theory for a physical quantity*, *Nucl. Phys.* **B 405** (1993) 424 [INSPIRE].

JHEP01(2013)125

[37] D.J. Broadhurst, *Large-N expansion of QED: asymptotic photon propagator and contributions to the muon anomaly, for any number of loops*, *Z. Phys.* **C 58** (1993) 339 [INSPIRE].

[38] A.H. Mueller, *On the structure of infrared renormalons in physical processes at high-energies*, *Nucl. Phys.* **B 250** (1985) 327 [INSPIRE].

[39] M. Beneke, *Renormalization scheme invariant large order perturbation theory and infrared renormalons in QCD*, *Phys. Lett.* **B 307** (1993) 154 [INSPIRE].

[40] D. Boito et al., *Duality violations in τ hadronic spectral moments*, *Nucl. Phys. Proc. Suppl.* **218** (2011) 104 [arXiv:1011.4426] [INSPIRE].

[41] A. Pich and J. Prades, *Strange quark mass determination from Cabibbo suppressed τ decays*, *JHEP* **10** (1999) 004 [hep-ph/9909244] [INSPIRE].

[42] E. Gámiz, M. Jamin, A. Pich, J. Prades and F. Schwab, *Determination of m_s and $|V_{us}|$ from hadronic τ decays*, *JHEP* **01** (2003) 060 [hep-ph/0212230] [INSPIRE].

[43] E. Gámiz, M. Jamin, A. Pich, J. Prades and F. Schwab, *V_{us} and m_s from hadronic τ decays*, *Phys. Rev. Lett.* **94** (2005) 011803 [hep-ph/0408044] [INSPIRE].

[44] M.A. Shifman, A.I. Vainshtein and V.I. Zakharov, *QCD and resonance physics. Sum rules*, *Nucl. Phys.* **B 147** (1979) 385 [INSPIRE].

[45] M. Jamin, *Flavor symmetry breaking of the quark condensate and chiral corrections to the Gell-Mann-Oakes-Renner relation*, *Phys. Lett.* **B 538** (2002) 71 [hep-ph/0201174] [INSPIRE].

[46] Particle Data Group collaboration, J. Beringer et al., *Review of particle physics*, *Phys. Rev.* **D 86** (2012) 010001 [INSPIRE].

JHEP01(2013)125